Physical Chemistry Chemical Physics: Supplementary Information (SI)

Title: Hydration-induced dynamical changes in lyophilised and weakly hydrated apoferritin: insights from Molecular Dynamics Simulation

Authors: Elisa Bassotti [1], Gaio Paradossi [1], Ester Chiessi *[1] and Mark Telling *[2,3]

Affiliations:

[1] Department of Chemical Science and Technologies, University of Rome Tor Vergata, Via della Ricerca Scientifica I, 00133, Rome, ITALY

[2] STFC, ISIS Facility, Rutherford Appleton Laboratory, Harwell Campus, OX11OQX, UK

[3] Department of Materials, University of Oxford, Parks Road, Oxford, UK

*corresponding authors

Sections

SI.1 Trajectory Analyses

SI.1.1 Root Mean Squared Deviation (RMSD)

To verify system equilibration, the structural evolution of lyophilised and weakly hydrated apoferritin was monitored by means of the Root Mean Squared Deviation (RMSD) of protein heavy atoms, whose time behaviour at 290 K is shown in Figure SI.1. The curves approximately reach a steady state at long times, confirming that equilibration has been reached. RMSD values are consistently lower for the lyophilised system.

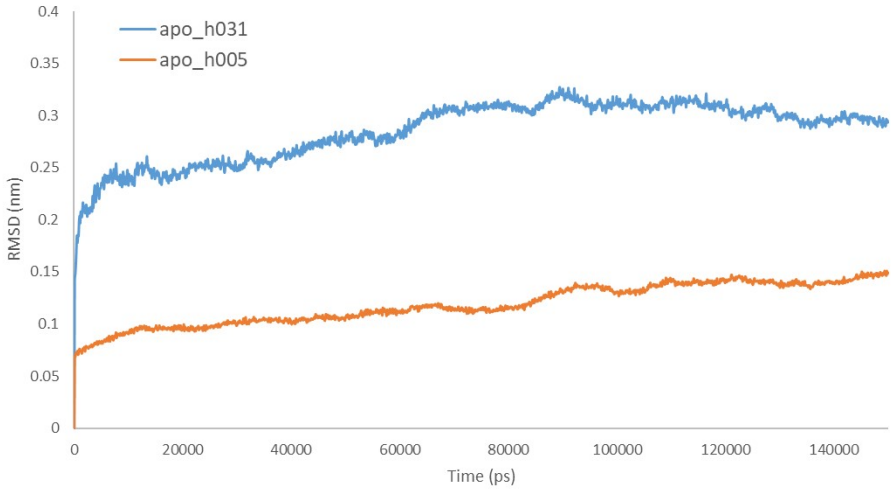

Figure SI.1. RMSD as function of time for all heavy atoms of lyophilised (apo_h005, orange) and weakly hydrated (apo_h031, blue) apoferritin. The RMSD was calculated over the whole NVT trajectory at 290 K.

SI.1.2 MSD per residue

The reproducibility of the dynamical response of apoferritin was verified by comparing the original simulation with an independent replica. Comparison was performed at the residue-resolved level. The MSD per residue values at 290 K at 150 K for the weakly hydrated and lyophilised protein, obtained from the last two 10 ns trajectory interval of both simulations, are consistent within 10%. Similarly, the reliability of the chosen sampling window (i.e., the last 20 ns of the trajectories) was assessed by performing the residue-resolved analysis of the mobility over the last 40 ns of the trajectories, dividing

this interval into four blocks of 10 ns each. The resulting MSD per residue values agree with those obtained from the two 10 ns blocks within 4%, thus validating our sampling strategy. These checks support the validity of results presented in this work.

Additionally, the COM motion of the biological assembly was monitored in order to establish whether such global motion would significantly influence the more localized MSD(t) behaviour of the protein hydrogen atoms. Results of this analysis are reported in detail in *Supplementary Methods 1.3: Centre of Mass Motion (COM) of the biological assembly* of the Supplementary Information of our previous work[1]. From this analysis the influence of COM motion on the average MSD of apoferritin hydrogen atoms results to be lower than 2% for both systems, a contribution that can be considered minor. Taking into account that the MSD per residue values are computed with an average over the 24 protein subunits, this test holds also for the determination of the MSD per residue values, therefore they were calculated with no trajectory correction.

SI.1.3 Classification of residues according to change in mobility (%) upon hydration

Concerning the classification of amino acids in terms of change in mobility (%) upon hydration, our rationale was as follows:

- Residues showing a mobility change between -10 and +10 % were considered unaffected by hydration. At this level, the change was deemed negligible and within error
- Residues showing a mobility change <-10% were considered as showing a hindering effect that was beyond standard error
- Residues showing a mobility change >+10% were considered to exhibit enhanced mobility beyond error
- The threshold used to define those residues exhibiting greatly enhanced mobility (i.e., >+60%) was chosen based on the overall distribution of detected mobility changes. Specifically, this threshold represents an enhancement exceeding the average change in mobility (%) upon hydration value by three standard errors, excluding residues with extreme enhancement from the statistical analysis.

SI.1.4 Radial Distribution Functions (RDFs)

The radial distribution of a specie, or species, around a reference position is described by the Radial Distribution Function (RDF):

$$RDF(r) = \frac{\langle \rho(r) \rangle}{\langle \rho_{local} \rangle} \qquad \textit{(Eq.SI.1)}$$

Here, $\langle \rho(r) \rangle$ represents the density of the specie(s) at a spherical distance *r* from a point of reference and $\langle \rho_{local} \rangle$ denotes the density of said specie(s) within a sphere centered at the reference position (with a radius r_{max} equal to half the box length). The reference position can correspond to a specific class of atoms or the center of mass (COM) of a group of atoms.

RDF analysis was performed to investigate how different species, namely methyl and non-methyl hydrogen atoms, hydrogens of residues with hindered mobility at 150 K and hydrogens of residues with greatly enhanced mobility at 290 K, are located with respect to water molecules. RDFs of each of the aforementioned species were compared to the RDF of water's atoms at the corresponding temperature. Each RDF was calculated using the last 10 ns of the 150 K or 290 K NVT trajectories of weakly hydrated apoferritin. When calculating RDFs of protein's atoms, only hydrogens were included; on the other hand, all atoms were selected for water's RDF calculation. All RDFs were calculated using the COM of the protein as the point of reference.

SI.1.5 Protein-water hydrogen bonds

First, the protein-water hydrogen bonds in the weakly hydrated system were analysed over the last 40 ns of the NVT trajectories (divided into two blocks of 20 ns each), using the geometric criteria of an acceptor-donor distance <0.35 nm and a hydrogen-donor-acceptor angle <30°. From this analysis, the total number of protein-water hydrogen bonds and their intermittent autocorrelation function, $C_H(t)$, were obtained.

The total number of protein-water hydrogen bonds was calculated as a function of temperature in the range 100-290 K. Results and errors are averages and standard deviations calculated over the last and second-to-last 20 ns of each trajectory, respectively.

The time decay of the intermittent autocorrelation function $C_H(t)$ of water-protein hydrogen bonds, defined in the Methods Section of the main text, is shown in Figure SI.2 for the range 225-290 K.

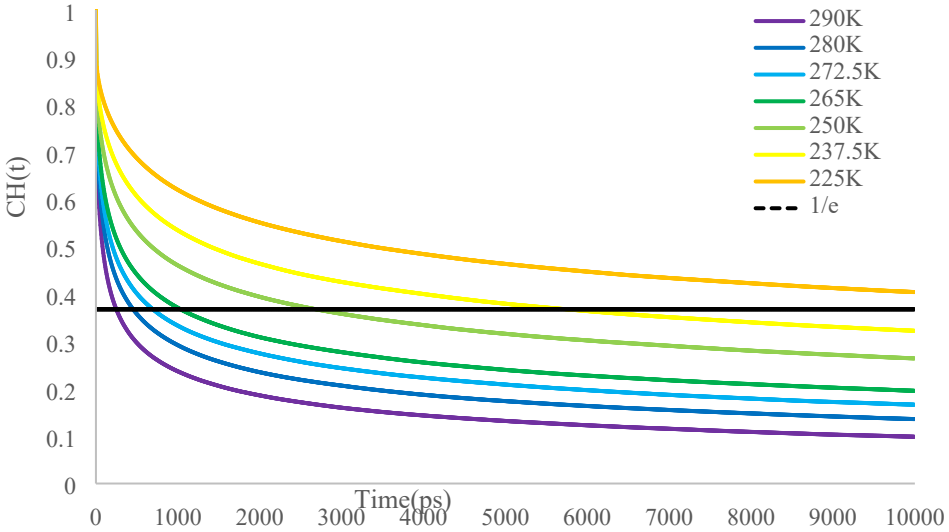

Figure SI.2. Autocorrelation function, $C_H(t)$, of the protein-water hydrogen bonds in apo_h031 in the temperature range 225-290 K. The characteristic lifetime, τ_H, of protein-water hydrogen bonds, is defined as the time when $C_H(t)$ reaches e^{-1} (horizontal dashed line).

To further characterise the protein-water interaction, the number of hydrogen bonds formed by each residue for more than 20% of the 290 and 150 K 10 ns trajectories, even if only intermittently (i.e., not continuously present in each 5 ps sampled frame of the 10 ns trajectory but instead making and breaking at various times), was calculated using the Python library MDAnalysis[2,3]. The python script used counted the total number of hydrogen bonds formed by unique combinations of donor, hydrogen and acceptor atoms and appearing, in total, in more than 20% of frames. The result for each amino acid was given by the sum of the number of hydrogen bonds identified for the same residue number in each of the 24 subunits. The geometric cutoffs of an acceptor-donor distance <0.35 nm and a hydrogen-donor-acceptor angle <30° were used. The analysis was performed for the last and second-to-last 10 ns production runs at 150 and 290 K. Results and errors are averages and standard deviations, respectively, from the two 10 ns intervals.

SI.1.6 Backbone vs. side-chain contributions to MSD

An MSD per residue analysis was carried out for backbone and side-chain hydrogen atoms separately. The analysis was performed as the whole residue analysis described in section SI.1.2, averaging the MSD vs time response in the last and second-to-last 10 ns intervals of the 150 K and 290 K trajectories over the 6-8 ns time range, this time considering separately hydrogen atoms belonging to backbone and side-chains. The residue-specific MSD value is obtained averaging over all 24 subunits. Results and errors are averages and standard deviations, respectively, from the two 10 ns production runs.

SI.1.7 Verification of the pseudo-symmetry assumption in residue-wise analyses

The results presented in this work were obtained by averaging MSD per residue values over the 24 subunits. To assess the validity of the assumption that using the average parameter is truly representative of an individual residue's behaviour, the MSD parameter was calculated for individual residues in each of the 24 subunits at 150 K and 290 K. Averages and standard deviations were then calculated for each residue over the 24 subunits, and the number of residues showing $MSD < MSD_{average} - 3 \cdot SD$ or $MSD > MSD_{average} + 3 \cdot SD$ was considered. Considering each of the 170 residues in the 24 subunits, only one subunit at most has an MSD value falling outside the range $MSD_{average} \pm 3 \cdot SD$. The total percentage of residues showing this kind of behaviour is lower than 3% (total number of residues = $24 \cdot 170$).

SI.1.8 Comparison between residue-wise Root Mean Squared Fluctuation and Mean Squared Displacement parameters

Considering the Gaussian approximation, mean squared displacement (MSD) and mean squared fluctuation values should be proportional. As a result, comparable results for MSD and root mean squared fluctuation (RMSF) are expected. To demonstrate this, RMSF(T) values of all apoferritin hydrogen atoms were calculated as a function of temperature for both lyophilised and weakly hydrated states. The interval chosen for the calculation was the range 6-8 ns of the last and second-to-last 10 ns, which corresponds to the time interval over which the MSD(T) was calculated. In Figure SI.3 RMSF(T)

results are compared to MSD(T) results. Comparison shows that the two dynamical observables follow similar trends, in particular concerning the low-temperature water-induced hindrance and the higher temperature dynamical transition. It can therefore be concluded that the MSD and RMSF parameters provide comparable information regarding protein mobility. As a result, the MSD parameter was chosen, since it is not only comparable to RMSF(T) but also a dynamic observable which can be accessed directly through neutron scattering experiments and, thus, provide an experimental reference for simulations reported in our previous work[1].

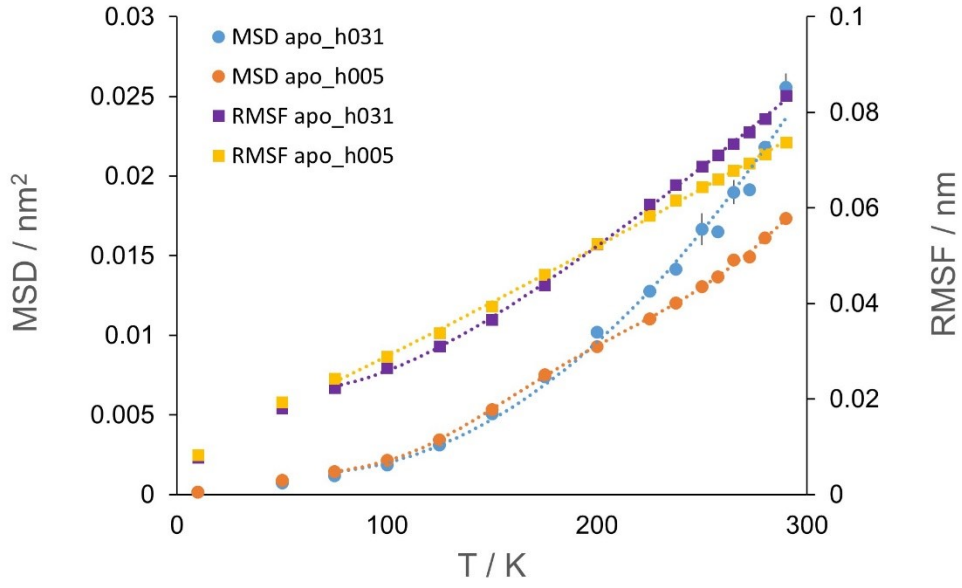

Figure SI.3. MSD (circles) and RMSF (squares) as a function of temperature for hydrogen atoms of apo_h031 and apo_h005. Dotted lines are a guide to the eye. Results and error bars were obtained from analysis of the last and second-to-last 10 ns production runs. Where not visible, error bars are within symbol size.

SI.2 MSD per residue results

SI.2.1 MSD per residue values

The residue-wise MSD parameters for lyophilised (apo_h005) and weakly hydrated (apo_h031) apoferritin at 290 K and 150 K along the primary sequence are reported in Figures SI.4 and SI.5,

respectively. Each residue is also associated with a bar whose colour highlights the relative effect of hydration on its displacement amplitude (according to the classification, based on Eq.3 of the main text, reported in Table 2 of the main text): hindrance (blue), negligible effect (grey), moderate enhancement (yellow), great enhancement (red).

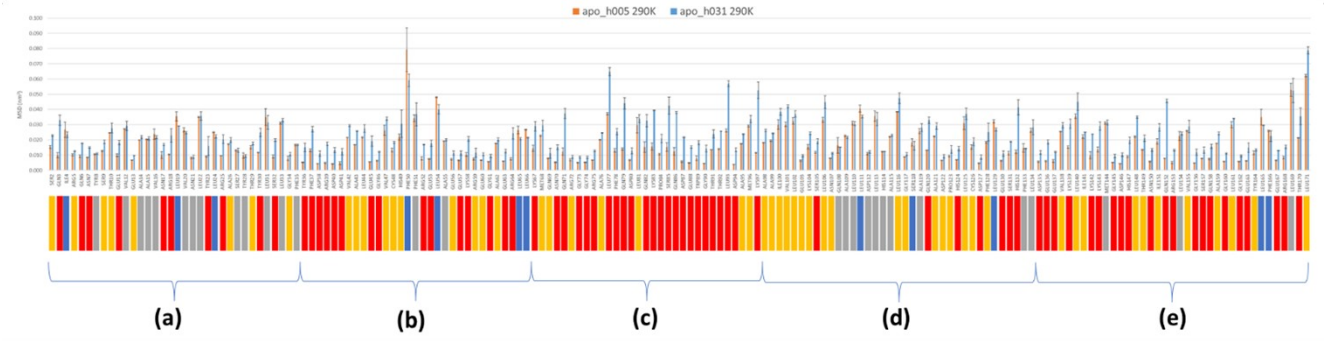

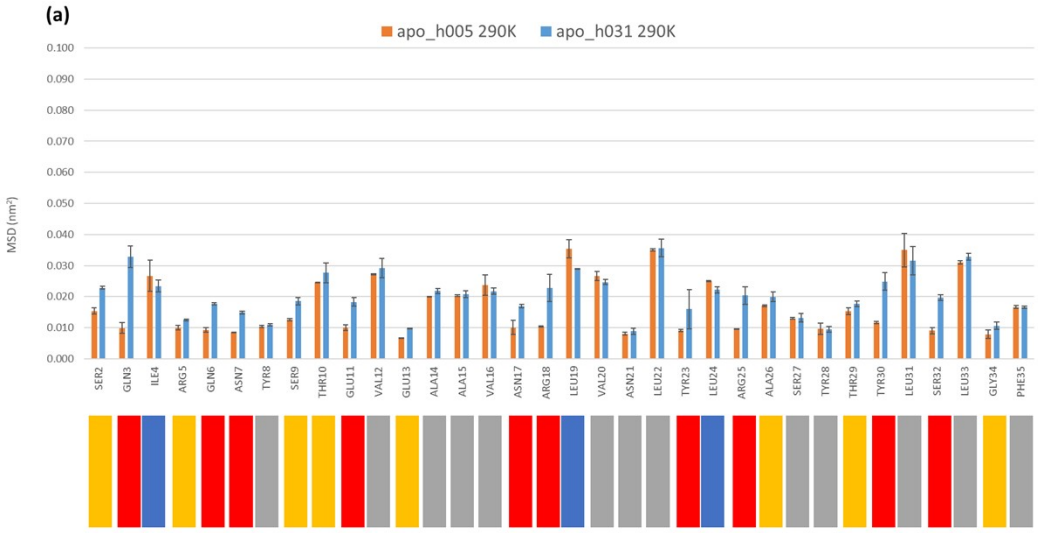

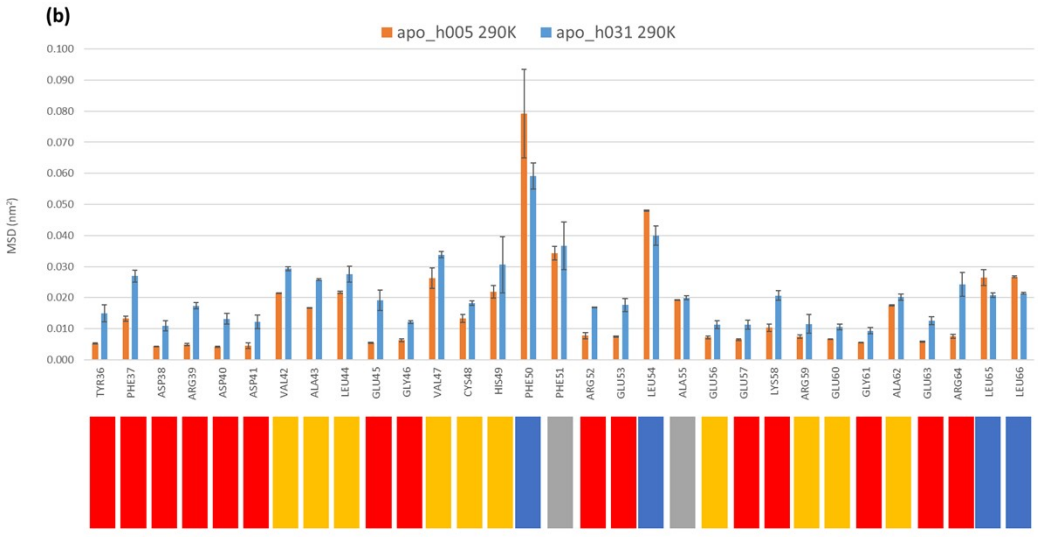

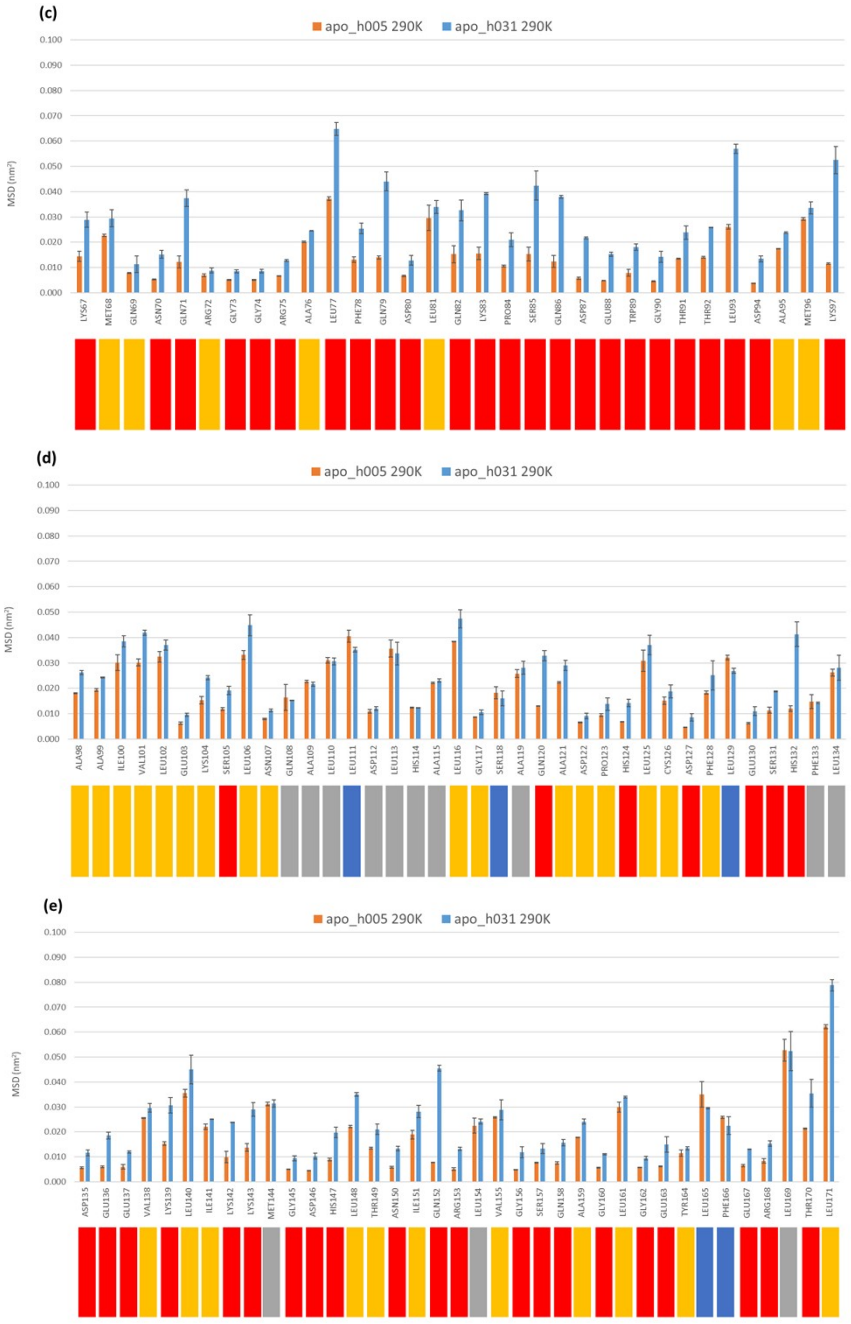

Figure SI.4. MSD per residue values along the primary sequence of apoferritin in the lyophilised (apo_h005, orange) and weakly hydrated (apo_h031, blue) states, at 290 K. Results and error bars were obtained from analysis of the last and second-to-last 10 ns of the trajectories, as averages and standard deviations, respectively. The sequence is divided into 5 regions, (a)-(e), to aid visualization. Each residue is also associated with a bar whose colour highlights the relative effect of hydration on its displacement amplitude: hindrance (blue), negligible effect (grey), moderate enhancement (yellow), great enhancement (red).

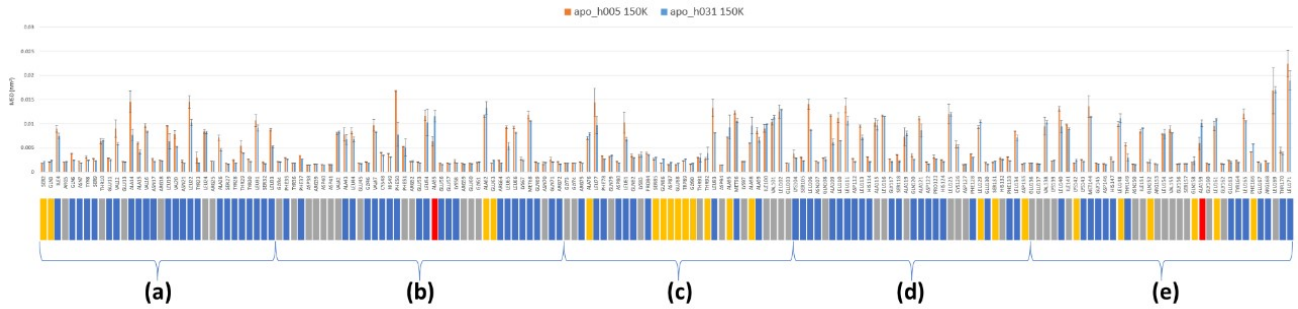
apo_h005 150K
apo_h031 150K
(a)
(b)
(c)
(d)
(e)

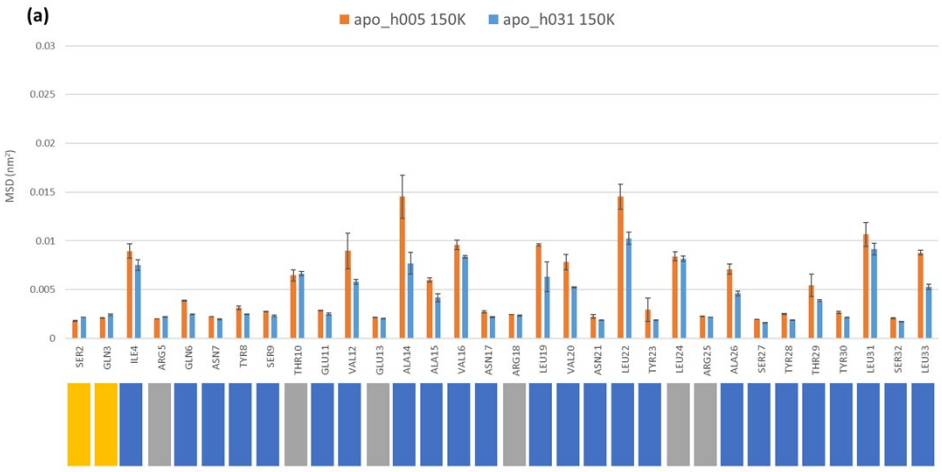
(a)
apo_h005 150K
apo_h031 150K
MSD (nm²)
0.03
0.025
0.02
0.015
0.01
0.005
0
SER2
GLN3
ILE4
ARG5
GLN6
ASN7
TYR8
SER9
THR10
GLU11
VAL12
GLU13
ALA14
ALA15
VAL16
ASN17
ARG18
LEU19
VAL20
ASN21
LEU22
TYR23
LEU24
ARG25
ALA26
SER27
TYR28
THR29
TYR30
LEU31
SER32
LEU33

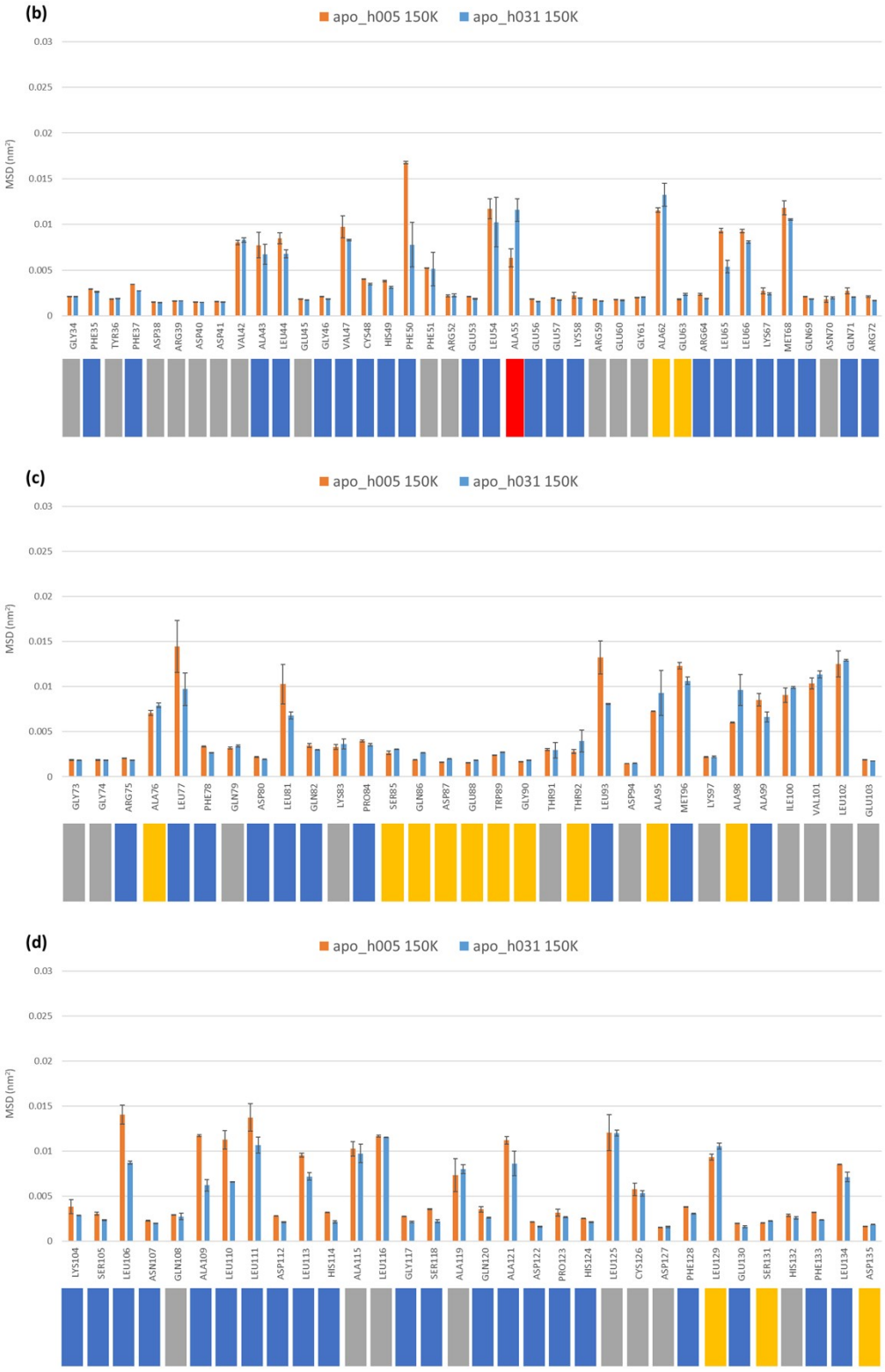
(b)
apo_h005 150K
apo_h031 150K
MSD (nm²)
0.03
0.025
0.02
0.015
0.01
0.005
0
GLY34 PHE35 TYR36 PHE37 ASP38 ARG39 ASP40 ASP41 VAL42 ALA43 LEU44 GLU45 GLY46 VAL47 CYS48 HIS49 PHE50 PHE51 ARG52 GLU53 LEU54 ALA55 GLU56 GLU57 LYS58 ARG59 GLU60 GLY61 ALA62 GLU63 ARG64 LEU65 LEU66 LYS67 MET68 GLN69 ASN70 GLN71 ARG72
(c)
apo_h005 150K
apo_h031 150K
MSD (nm²)
0.03
0.025
0.02
0.015
0.01
0.005
0
GLY73 GLY74 ARG75 ALA76 LEU77 PHE78 GLN79 ASP80 LEU81 GLN82 LYS83 PRO84 SER85 GLN86 ASP87 GLU88 TRP89 GLY90 THR91 THR92 LEU93 ASP94 ALA95 MET96 LYS97 ALA98 ALA99 ILE100 VAL101 LEU102 GLU103
(d)
apo_h005 150K
apo_h031 150K
MSD (nm²)
0.03
0.025
0.02
0.015
0.01
0.005
0
LYS104 SER105 LEU106 ASN107 GLN108 ALA109 LEU110 LEU111 ASP112 LEU113 HIS114 ALA115 LEU116 GLY117 SER118 ALA119 GLN120 ALA121 ASP122 PRO123 HIS124 LEU125 CYS126 ASP127 PHE128 LEU129 GLU130 SER131 HIS132 PHE133 LEU134 ASP135

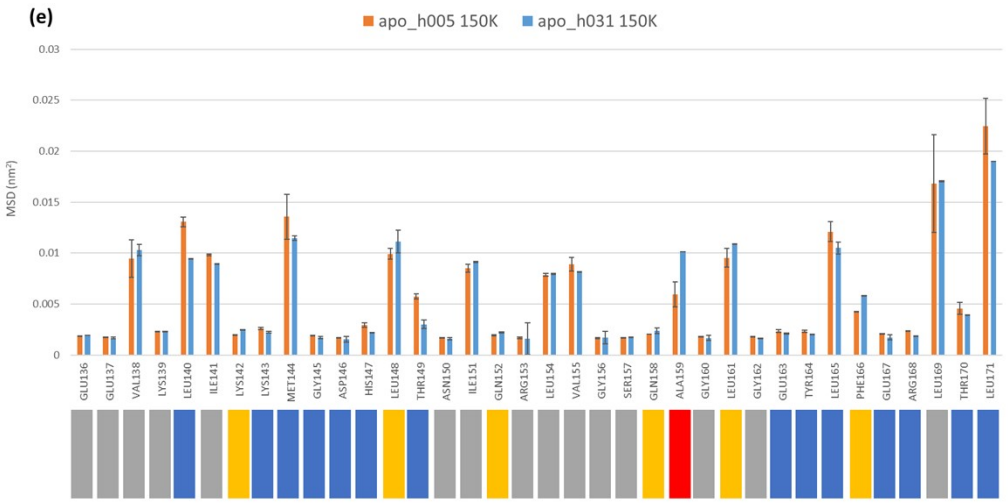

Figure SI.5. MSD per residue values along the primary sequence of apoferritin in the lyophilised (apo_h005, orange) and weakly hydrated (apo_h031, blue) states, at 150 K. Results and error bars were obtained from analysis of the last and second-to-last 10 ns of the trajectories, as averages and standard deviations, respectively. The sequence is divided into 5 regions, (a)-(e), to aid visualization. Each residue is also associated with a bar whose colour highlights the relative effect of hydration on its displacement amplitude: hindrance (blue), negligible effect (grey), moderate enhancement (yellow), great enhancement (red).

SI.2.2 Change in mobility (%) upon hydration values

The percentage changes in MSD upon hydration, calculated according to Eq.3 (main text), are reported for all residues at 290 K and 150 K in Figures SI.6 and SI.7, respectively.

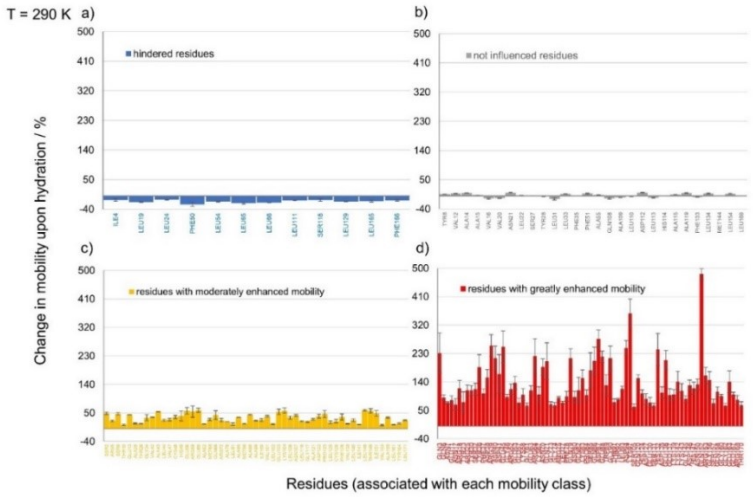

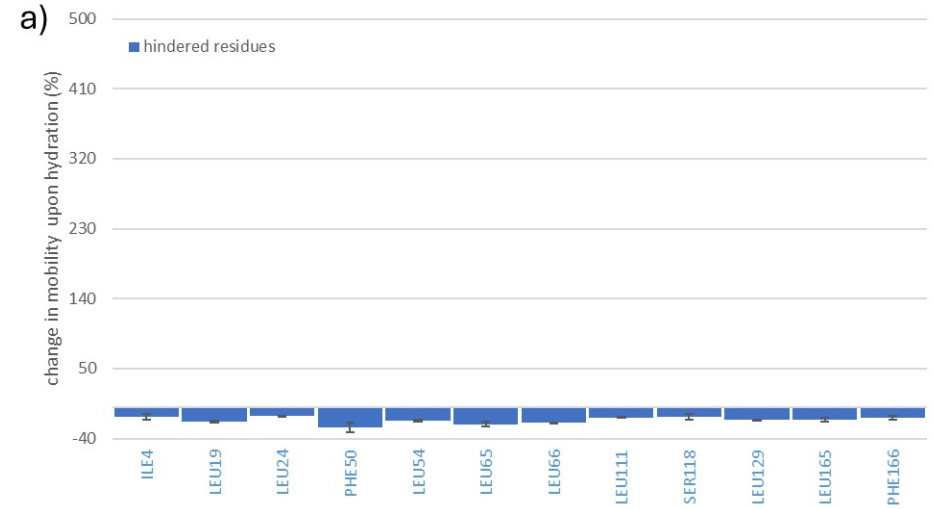
a)
hindered residues
change in mobility upon hydration (%)
500
410
320
230
140
50
-40
ILE4
LEU19
LEU24
PHE50
LEU54
LEU65
LEU66
LEU111
SER118
LEU129
LEU165
PHE166

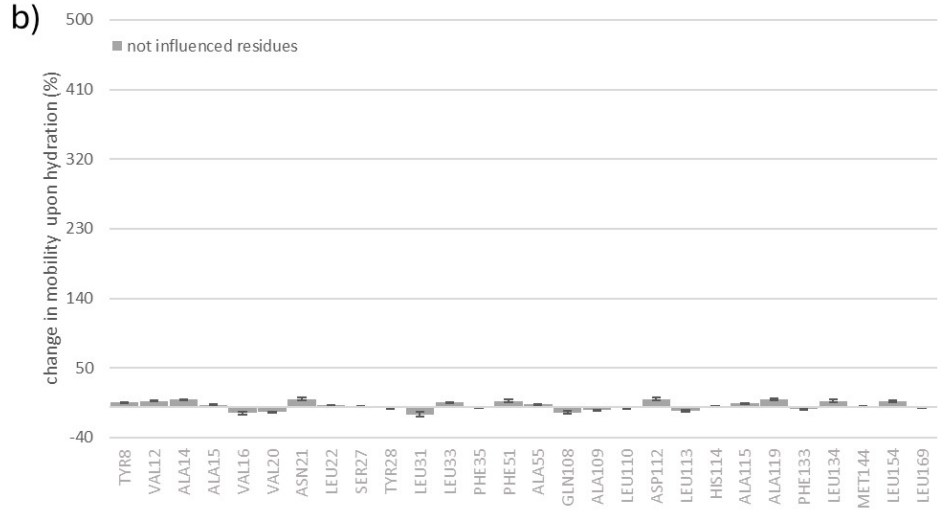
b)
not influenced residues
change in mobility upon hydration (%)
500
410
320
230
140
50
-40
TYR8
VAL12
ALA14
ALA15
VAL16
VAL20
ASN21
LEU22
SER27
TYR28
LEU31
LEU33
PHE35
PHE51
ALA55
GLN108
ALA109
LEU110
ASP112
LEU113
HIS114
ALA115
ALA119
PHE133
LEU134
MET144
LEU154
LEU169

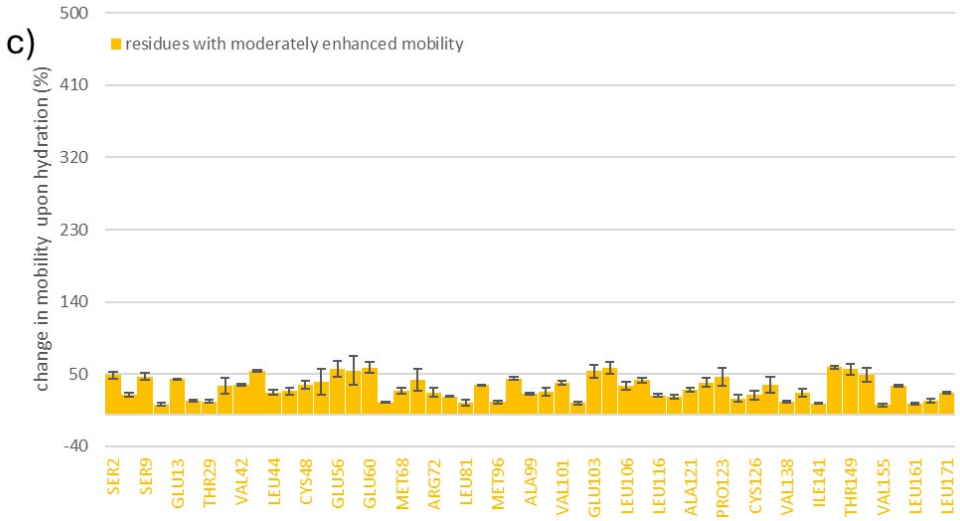
c)
residues with moderately enhanced mobility
change in mobility upon hydration (%)
500
410
320
230
140
50
-40
SER2
SER9
GLU13
THR29
VAL42
LEU44
CYS48
GLU56
GLU60
MET68
ARG72
LEU81
MET96
ALA99
VAL101
GLU103
LEU106
LEU116
ALA121
PRO123
CYS126
VAL138
ILE141
THR149
VAL155
LEU161
LEU171

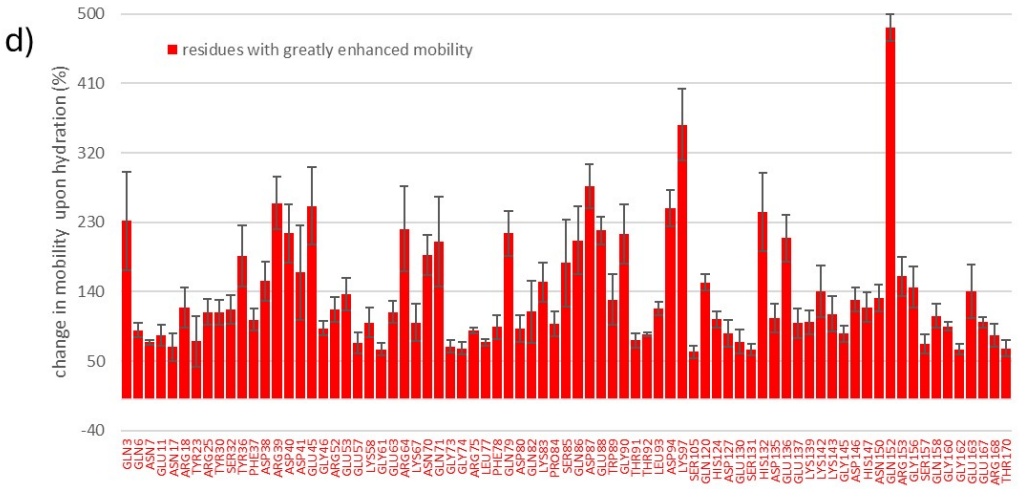

Figure SI.6. Change in mobility upon hydration (Eq. 3 in the main text) per residue at T = 290 K for a) hindered residues, b) not influenced residues, c) residues with moderately enhanced mobility, d) residues with greatly enhanced mobility upon hydration. Each panel displays results specific to a particular class of amino acids, with x-ticks representing only residues within that class.

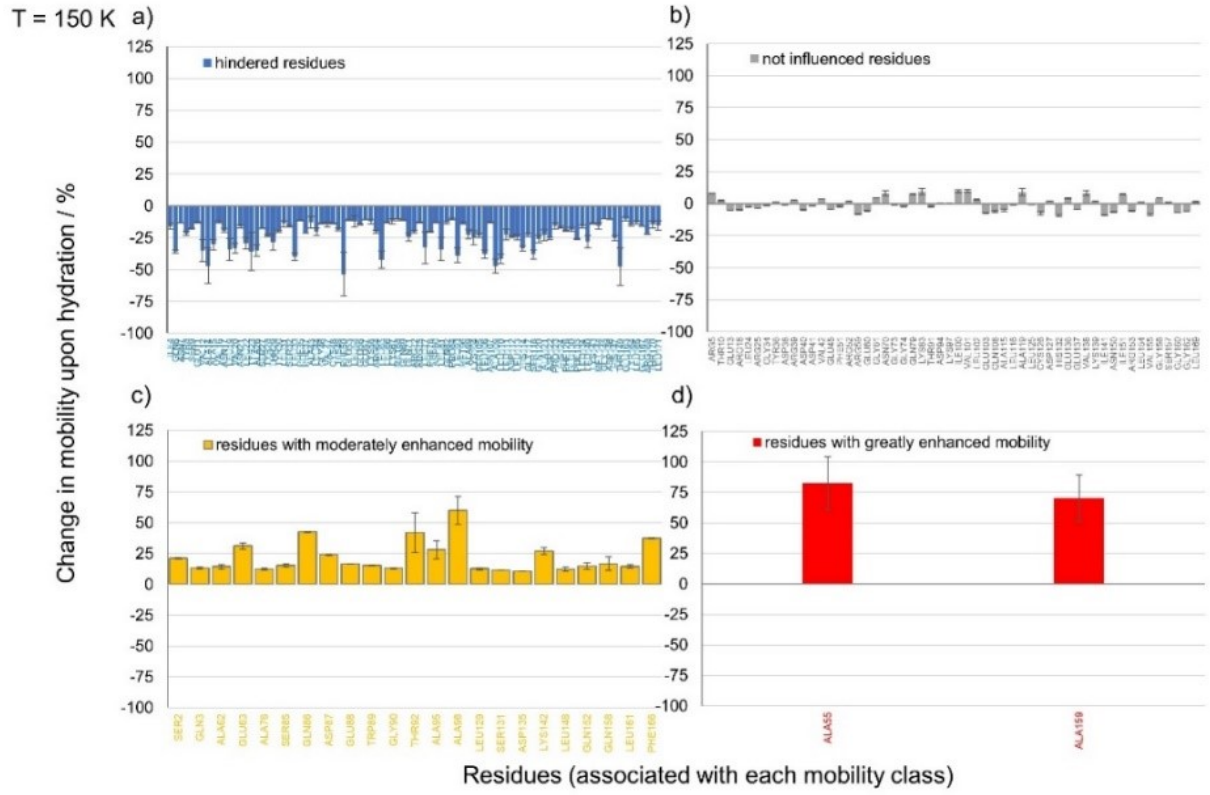

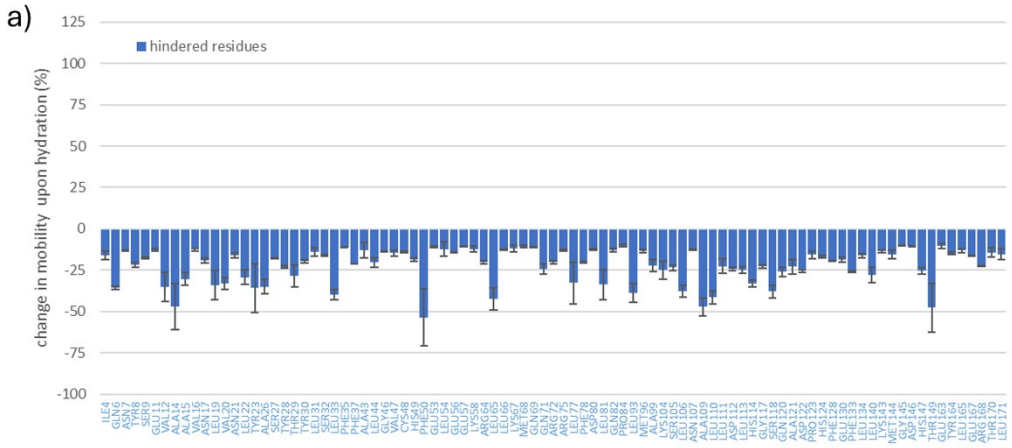
a)
hindered residues
change in mobility upon hydration (%)
125
100
75
50
25
0
-25
-50
-75
-100

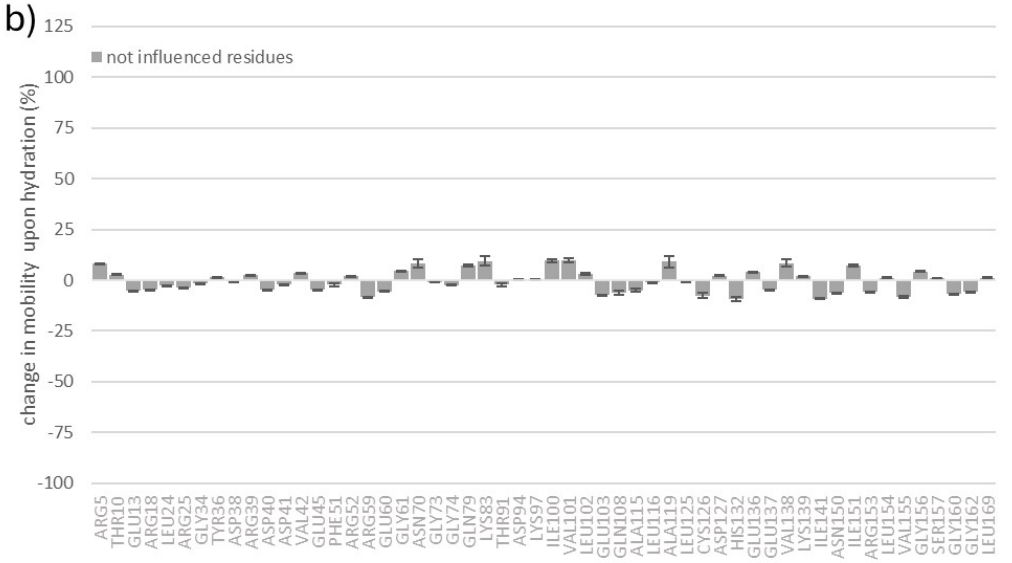
b)
not influenced residues
change in mobility upon hydration (%)
125
100
75
50
25
0
-25
-50
-75
-100
ARG5
THR10
GLU13
ARG18
LEU24
ARG25
GLY34
TYR36
ASP38
ARG39
ASP40
ASP41
VAL42
GLU45
PHE51
ARG52
ARG59
GLU60
GLY61
ASN70
GLY73
GLY74
GLN79
LYS83
THR91
ASP94
LYS97
ILE100
VAL101
LEU102
GLU103
GLN108
ALA115
LEU116
ALA119
LEU125
CYS126
ASP127
HIS132
GLU136
GLU137
VAL138
LYS139
ILE141
ASN150
ILE151
ARG153
LEU154
VAL155
GLY156
SER157
GLY160
GLY162
LEU169

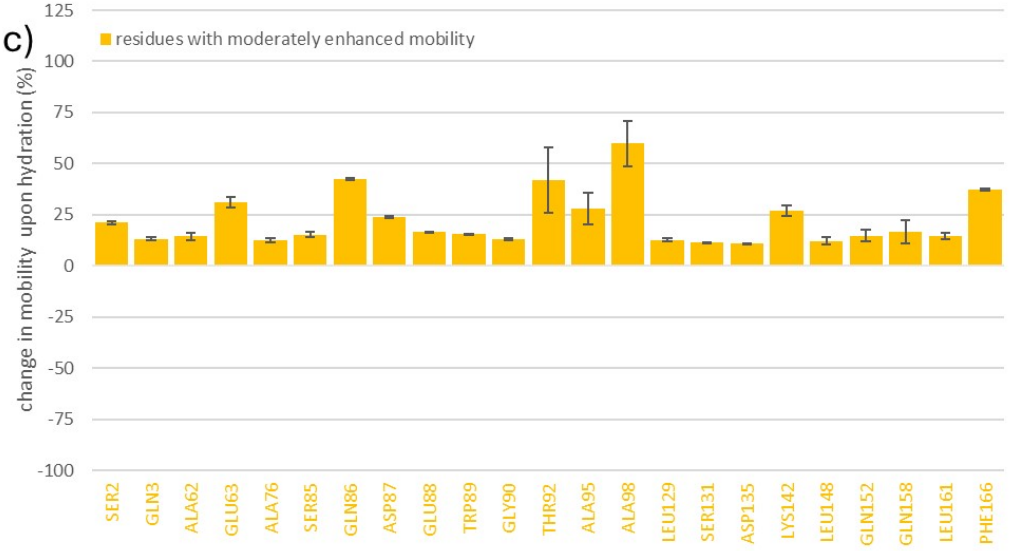
c)
residues with moderately enhanced mobility
change in mobility upon hydration (%)
125
100
75
50
25
0
-25
-50
-75
-100
SER2
GLN3
ALA62
GLU63
ALA76
SER85
GLN86
ASP87
GLU88
TRP89
GLY90
THR92
ALA95
ALA98
LEU129
SER131
ASP135
LYS142
LEU148
GLN152
GLN158
LEU161
PHE166

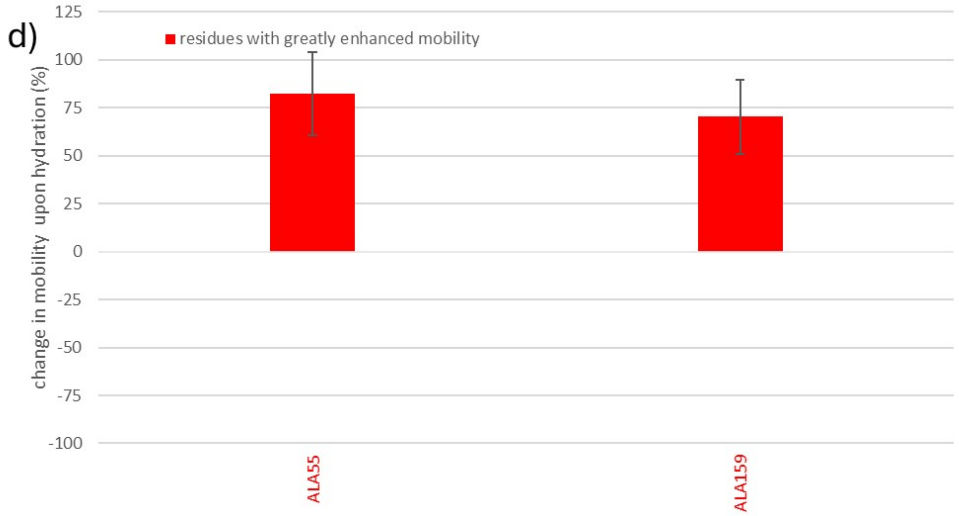

Figure SI.7. Change in mobility upon hydration (Eq. 3 in the main text) per residue at T = 150 K for a) hindered residues, b) not influenced residues, c) residues with moderately enhanced mobility, d) residues with greatly enhanced mobility upon hydration. Each panel displays results specific to a particular class of amino acids, with x-ticks representing only residues within that class.

SI.2.3 MSD per residue analysis with methyl rotation removal

The MSD per residue parameters and changes in mobility (%) upon hydration (Eq.3 of the main text) were also calculated using trajectories in which the rotation of methyl groups was removed[1], at 150 and 290 K. Considering that the extent of the rotational methyl motion is independent of the hydration level (Figure 4a of ref.1), its removal should not alter the results but increase the signal-to-noise ratio. Figures SI.8 and SI.9 display the changes in mobility (%) upon hydration along the primary structure, comparing the values obtained including and not including the methyl rotation motion. In general, the outcome of such analysis makes the temperature-dependent effects of hydration on mobility more evident. At 290 K, the number of residues with greatly enhanced mobility increases (Table SI.1), with methyl-containing residues now showing great mobility enhancement (Table SI.2), as opposed to the case of trajectories with methyl rotations. In a similar way, the hindrance effect at 150 K is accentuated in the trajectories without methyl rotations (Table SI.3), with the number of methyl-containing residues having hindered mobility increasing (Table SI.4). It is also noteworthy that with methyl rotation removal the great enhancement effect on methyl containing residues is no longer observed (the two ALA

residues that showed greatly enhanced mobility in the original trajectories (Figure 11d in the main manuscript) are hindered or unaffected when methyl rotation is removed).

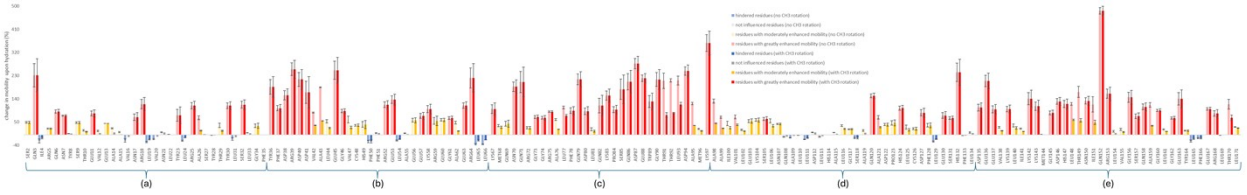

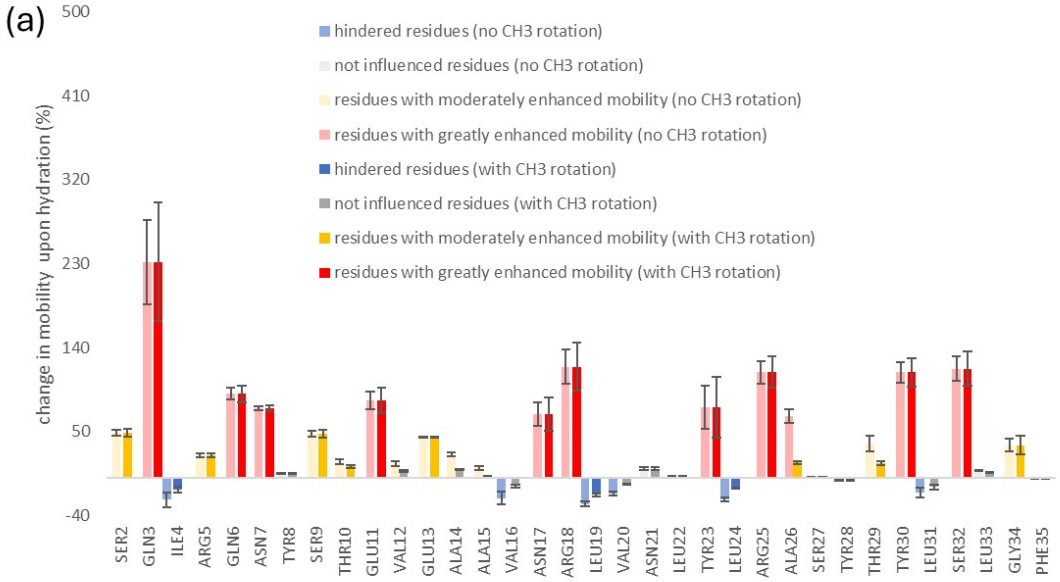

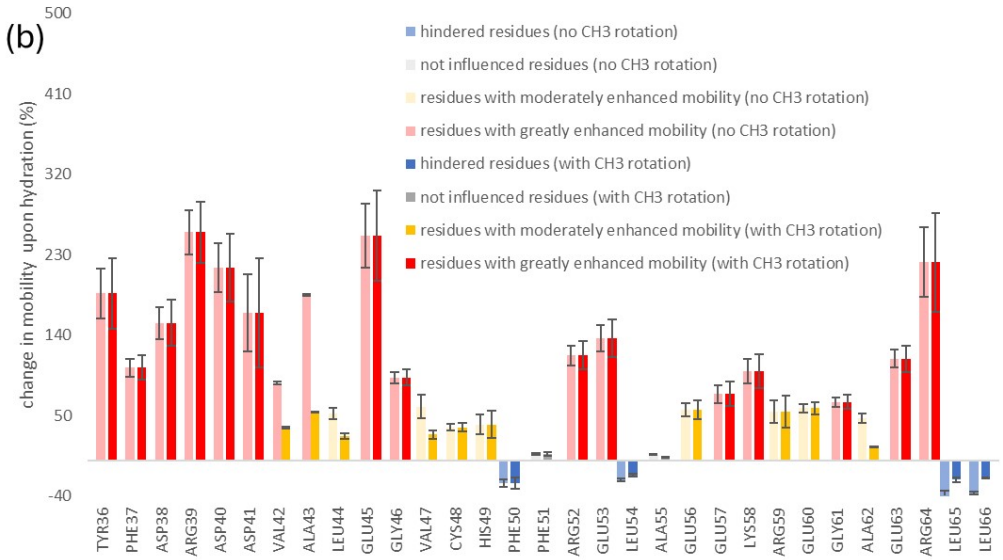

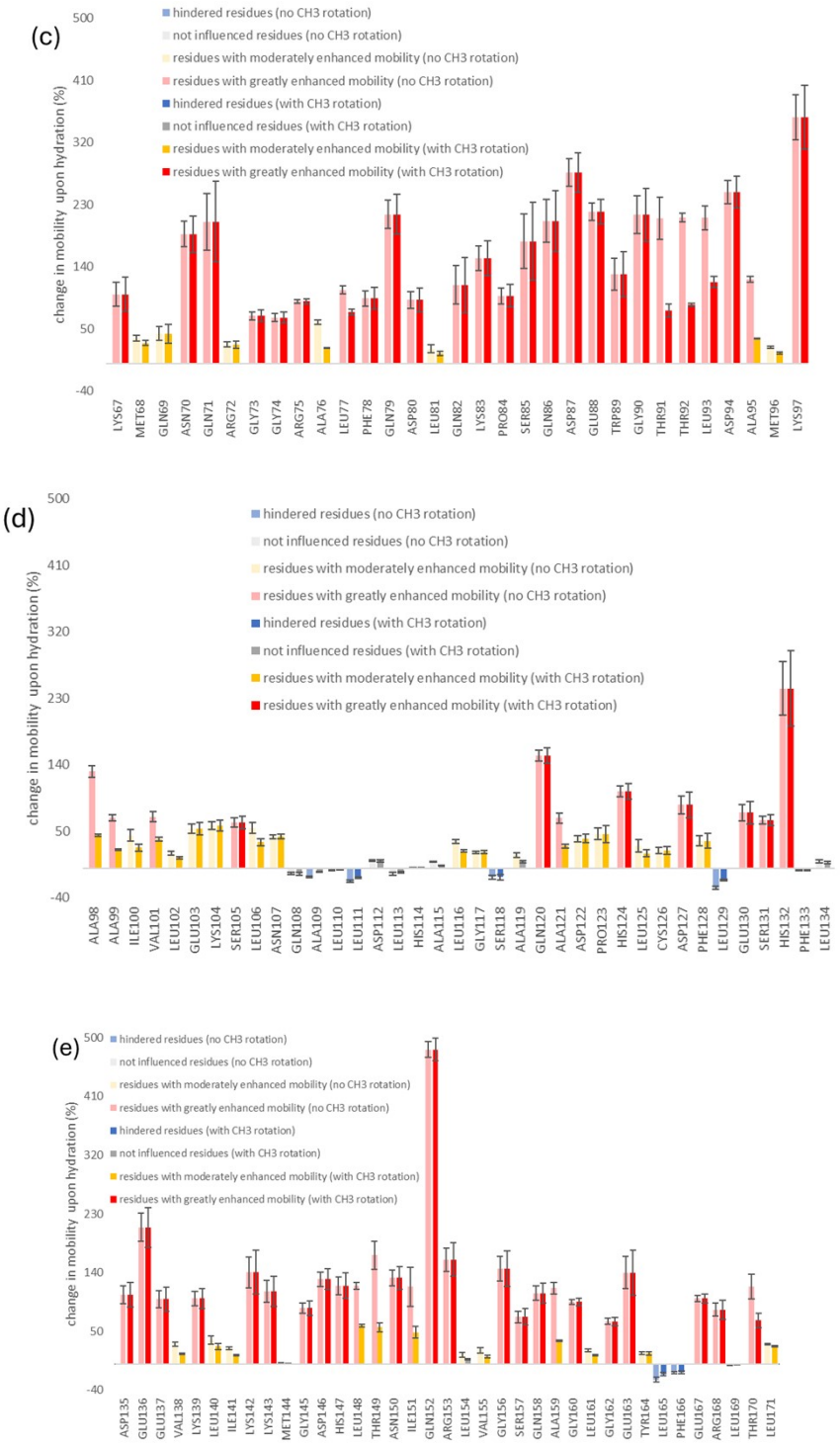

Figure SI.8. Change in mobility upon hydration (Eq. 3 in the main text) per residue at T = 290 K along the primary sequence for trajectory with (bright colours) and without (muted colours) methyl rotations. Bars are colour-coded to represent the hydration-induced effect: blue for hindrance, grey for negligible effect, yellow for moderate enhancement, and red for great enhancement. Results and error bars are derived from averages and standard deviations over the last and second-to-last 10 ns. The sequence is divided into 5 regions, (a)-(e), to aid visualization.

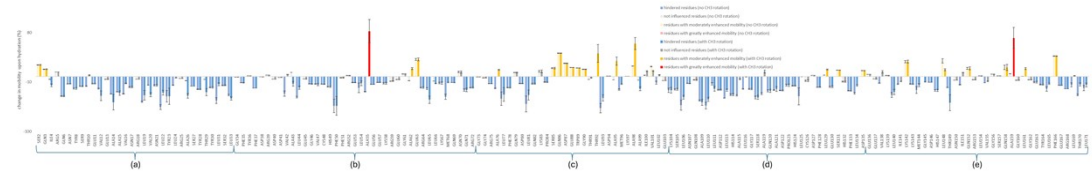

(a)

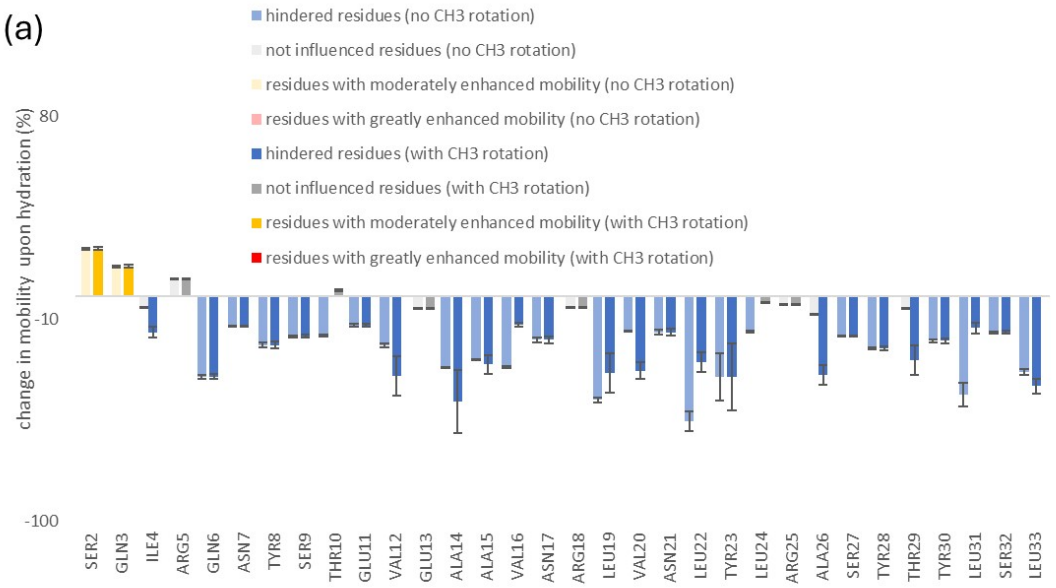
hindered residues (no CH3 rotation)
not influenced residues (no CH3 rotation)
residues with moderately enhanced mobility (no CH3 rotation)
residues with greatly enhanced mobility (no CH3 rotation)
hindered residues (with CH3 rotation)
not influenced residues (with CH3 rotation)
residues with moderately enhanced mobility (with CH3 rotation)
residues with greatly enhanced mobility (with CH3 rotation)
change in mobility upon hydration (%)
80
-10
-100
SER2 GLN3 ILE4 ARG5 GLN6 ASN7 TYR8 SER9 THR10 GLU11 VAL12 GLU13 ALA14 ALA15 VAL16 ASN17 ARG18 LEU19 VAL20 ASN21 LEU22 TYR23 LEU24 ARG25 ALA26 SER27 TYR28 THR29 TYR30 LEU31 SER32 LEU33

(b)

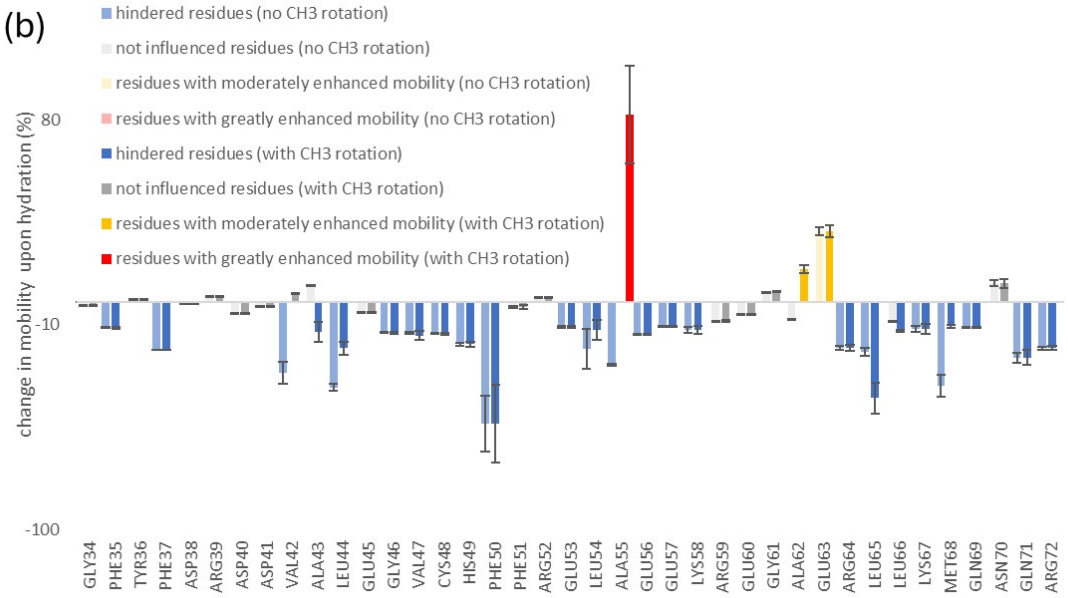
hindered residues (no CH3 rotation)
not influenced residues (no CH3 rotation)
residues with moderately enhanced mobility (no CH3 rotation)
residues with greatly enhanced mobility (no CH3 rotation)
hindered residues (with CH3 rotation)
not influenced residues (with CH3 rotation)
residues with moderately enhanced mobility (with CH3 rotation)
residues with greatly enhanced mobility (with CH3 rotation)
change in mobility upon hydration (%)
80
-10
-100
GLY34 PHE35 TYR36 PHE37 ASP38 ARG39 ASP40 ASP41 VAL42 ALA43 LEU44 GLU45 GLY46 VAL47 CYS48 HIS49 PHE50 PHE51 ARG52 GLU53 LEU54 ALA55 GLU56 GLU57 LYS58 ARG59 GLU60 GLY61 ALA62 GLU63 ARG64 LEU65 LEU66 LYS67 MET68 GLN69 ASN70 GLN71 ARG72

(c)

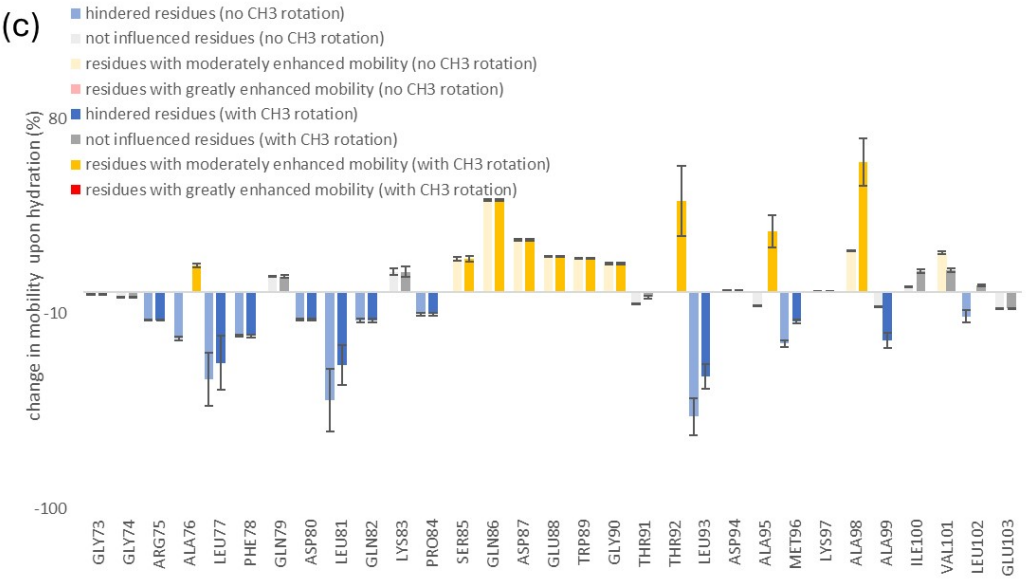
hindered residues (no CH3 rotation)
not influenced residues (no CH3 rotation)
residues with moderately enhanced mobility (no CH3 rotation)
residues with greatly enhanced mobility (no CH3 rotation)
hindered residues (with CH3 rotation)
not influenced residues (with CH3 rotation)
residues with moderately enhanced mobility (with CH3 rotation)
residues with greatly enhanced mobility (with CH3 rotation)
change in mobility upon hydration (%)
80
-10
-100
GLY73 GLY74 ARG75 ALA76 LEU77 PHE78 GLN79 ASP80 LEU81 GLN82 LYS83 PRO84 SER85 GLN86 ASP87 GLU88 TRP89 GLY90 THR91 THR92 LEU93 ASP94 ALA95 MET96 LYS97 ALA98 ALA99 ILE100 VAL101 LEU102 GLU103

(d)

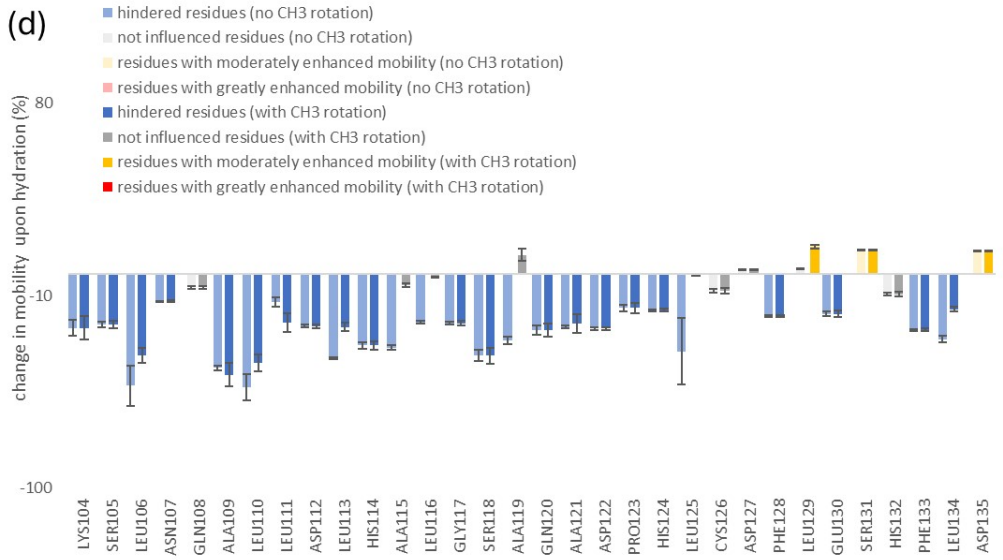
hindered residues (no CH3 rotation)
not influenced residues (no CH3 rotation)
residues with moderately enhanced mobility (no CH3 rotation)
residues with greatly enhanced mobility (no CH3 rotation)
hindered residues (with CH3 rotation)
not influenced residues (with CH3 rotation)
residues with moderately enhanced mobility (with CH3 rotation)
residues with greatly enhanced mobility (with CH3 rotation)
change in mobility upon hydration (%)
80
-10
-100
LYS104 SER105 LEU106 ASN107 GLN108 ALA109 LEU110 LEU111 ASP112 LEU113 HIS114 ALA115 LEU116 GLY117 SER118 ALA119 GLN120 ALA121 ASP122 PRO123 HIS124 LEU125 CYS126 ASP127 PHE128 LEU129 GLU130 SER131 HIS132 PHE133 LEU134 ASP135

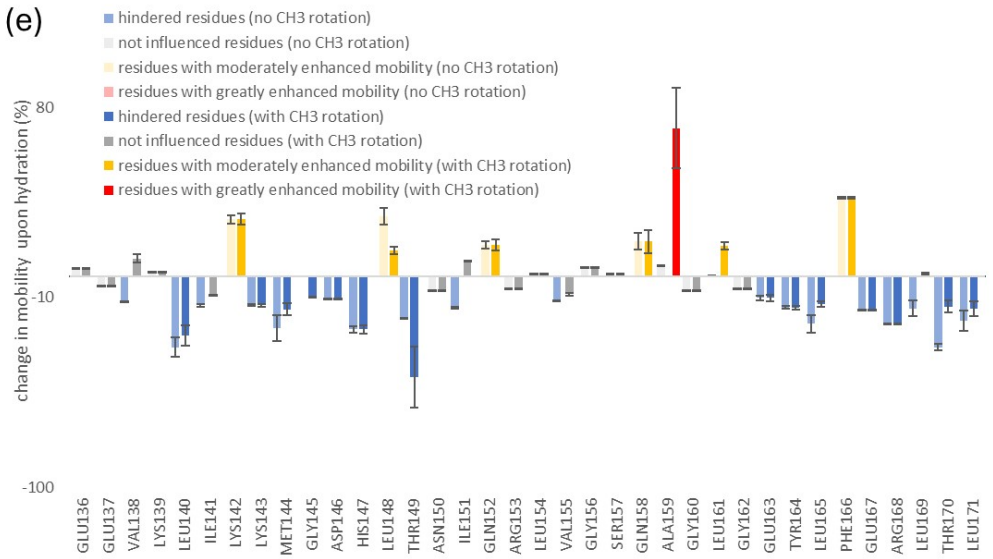

Figure SI.9. Change in mobility upon hydration (Eq. 3 in the main text) per residue at T = 150 K along the primary sequence for trajectory with (bright colours) and without (muted colours) methyl rotations. Bars are colour-coded to represent the hydration-induced effect: blue for hindrance, grey for negligible effect, yellow for moderate enhancement, and red for great enhancement. Results and error bars are derived from averages and standard deviations over the last and second-to-last 10 ns. The sequence is divided into 5 regions, (a)-(e), to aid visualization.

Table SI.1. Number and percentage of residues experiencing hindrance, negligible effect, moderate enhancement and great enhancement of mobility upon hydration at 290 K in the apoferritin subunit (total number of residues = 170) for trajectories with and without methyl rotations. Results are obtained averaging MSD per residue values over all 24 subunits. Errors are generated by analysing the last and second-to-last 10 ns intervals of the trajectory and determining a standard deviation (SD). Where errors are not reported, SD = 0 (indicating that the analysis on the two production runs gave identical results).

T = 290 K	*number of residues (with CH3 rotation)*	*number of residues (no CH3 rotation)*	*% of residues (with CH3 rotation)*	*% of residues (no CH3 rotation)*
hindrance	12 ± 2	16 ± 2	(7 ± 1) %	(9 ± 1) %
negligible effect	28 ± 3	19 ± 3	(17 ± 1) %	(11 ± 2) %
moderate enhancement	53 ± 5	46 ± 7	(31 ± 3) %	(27 ± 4) %
great enhancement	77 ± 9	89	(45 ± 5) %	52 %

Table SI.2. Number of methyl-containing residues in the apoferritin subunit (total number of residues = 170) showing each hydration-induced effect (hindrance, negligible effect, moderate enhancement, great enhancement) at 290 K in trajectories with and without methyl rotations. Results are obtained averaging MSD per residue values over all 24 subunits. Errors are generated by analysing the last and second-to-last 10 ns intervals of the trajectory and determining a standard deviation (SD). Where errors are not reported, SD = 0 (indicating that the analysis on the two production runs gave identical results).

T = 290 K	*number of **methyl-containing** residues (with CH3 rotation)*	*number of **methyl-containing** residues (no CH3 rotation)*
hindrance	9 ± 2	13 ± 2
negligible effect	17 ± 2	8 ± 2
moderate enhancement	30 ± 2	23 ± 1
great enhancement	5 ± 2	17

Table SI.3. Number and percentage of residues experiencing hindrance, negligible effect, moderate enhancement and great enhancement of mobility upon hydration at 150 K in the apoferritin subunit (total number of residues = 170) for trajectories with and without methyl rotations. Results are obtained averaging MSD per residue values over all 24 subunits. Errors are generated by analysing the last and second-to-last 10 ns intervals of the trajectory and determining a standard deviation (SD). Where errors are not reported, SD = 0 (indicating that the analysis on the two production runs gave identical results).

T = 150 K	*number of residues (with CH3 rotation)*	*number of residues (no CH3 rotation)*	*% of residues (with CH3 rotation)*	*% of residues (no CH3 rotation)*
hindrance	91 ± 1	99	54 %	58 %
negligible effect	54 ± 1	52 ± 2	32 %	(31 ± 1) %
moderate enhancement	23	18 ± 2	13 %	(11 ± 1) %
great enhancement	2 ± 1	0	1 %	0 %

Table SI.4. Number of methyl-containing residues in the apoferritin subunit (total number of residues = 170) showing each hydration-induced effect (hindrance, negligible effect, moderate enhancement, great enhancement) at 150 K in trajectories with and without methyl rotations. Results are obtained averaging MSD per residue values over all 24 subunits. Errors are generated by analysing the last and second-to-last 10 ns intervals of the trajectory and determining a standard deviation (SD). Where errors are not reported, SD = 0 (indicating that the analysis on the two production runs gave identical results).

T = 150 K	*number of **methyl-containing** residues (with CH3 rotation)*	*number of **methyl-containing** residues (no CH3 rotation)*
hindrance	34	43 ± 1
negligible effect	17 ± 2	15 ± 1
moderate enhancement	8 ± 2	23 ± 1
great enhancement	2 ± 1	0

SI.3 Backbone and Side Chain mobility analysis

SI.3.1 Backbone vs. side-chain contributions to MSD

An MSD per residue analysis was carried out for backbone and side-chain hydrogen atoms separately at 290 K and 150 K. Results are reported in Figures SI.10 (T=290 K) and SI.11 (T=150 K). At 290 K both systems show that the residue-wise MSD of the backbone is lower than that of the side chain for almost all residues. This result confirms the direct role of water in affecting the protein local mobility at this temperature, since the SASA and degree of hydration of side-chains are greater than the ones of the backbone (Figures SI.13a and SI.14). Comparing the mobility of dry and weakly hydrated apoferritin at 290 K, the residue-wise MSD for the backbone is always greater in the latter system. This trend generally extends to the side-chains as well, although there are some exceptions (the most evident examples are amino acids LEU19, PHE50, LEU54, LEU111, LEU156). It is interesting to note that these exceptions occur for amino acids with hydrophobic side chain and thus lower water affinity.

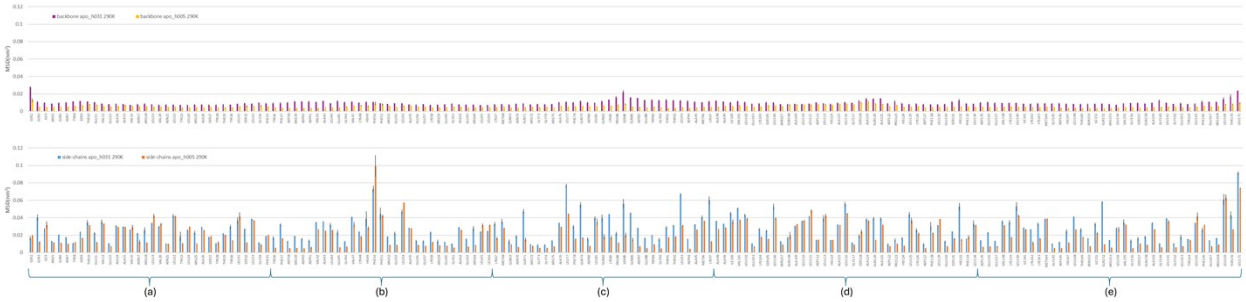
(a)
(b)
(c)
(d)
(e)

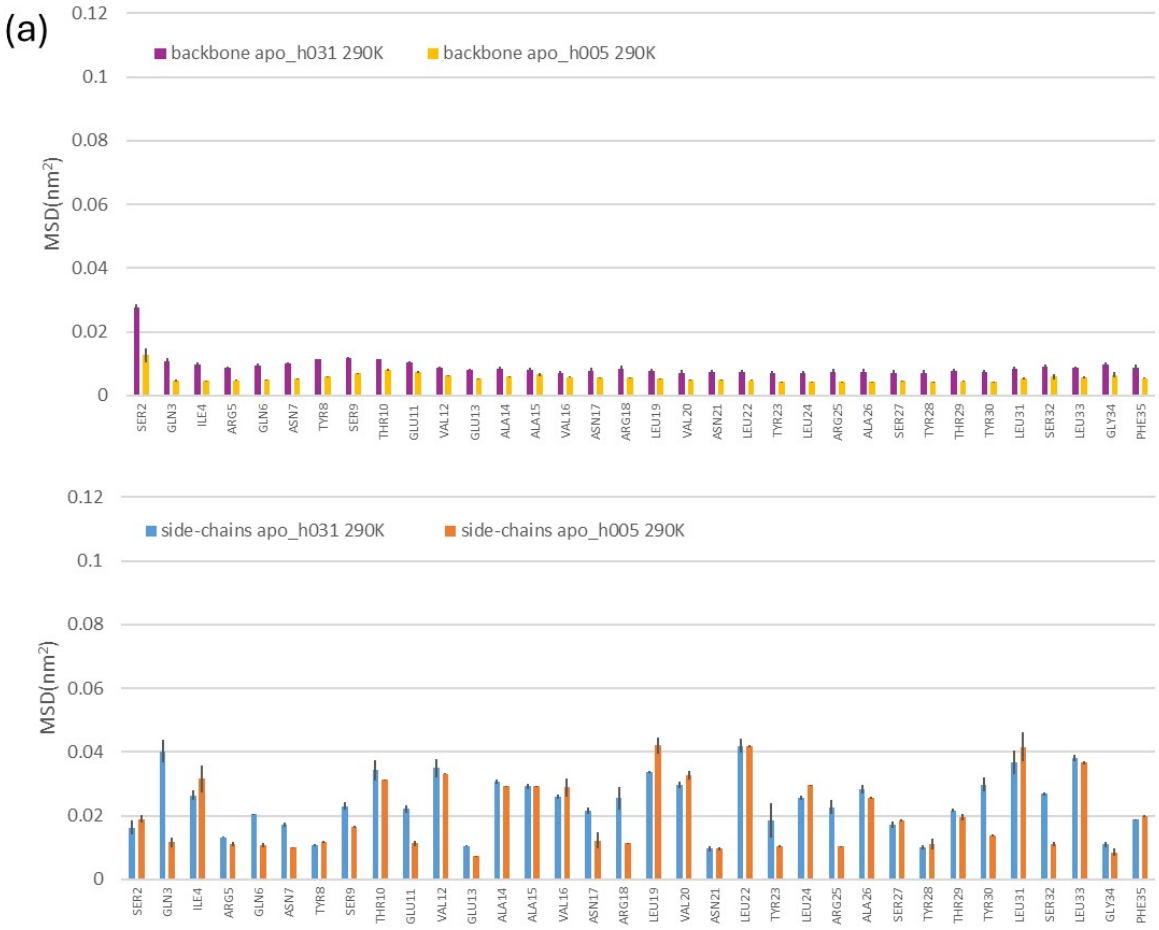
(a)
backbone apo_h031 290K
backbone apo_h005 290K
MSD(nm²)
0.12
0.1
0.08
0.06
0.04
0.02
0
SER2 GLN3 ILE4 ARG5 GLN6 ASN7 TYR8 SER9 THR10 GLU11 VAL12 GLU13 ALA14 ALA15 VAL16 ASN17 ARG18 LEU19 VAL20 ASN21 LEU22 TYR23 LEU24 ARG25 ALA26 SER27 TYR28 THR29 TYR30 LEU31 SER32 LEU33 GLY34 PHE35
side-chains apo_h031 290K
side-chains apo_h005 290K
MSD(nm²)
0.12
0.1
0.08
0.06
0.04
0.02
0
SER2 GLN3 ILE4 ARG5 GLN6 ASN7 TYR8 SER9 THR10 GLU11 VAL12 GLU13 ALA14 ALA15 VAL16 ASN17 ARG18 LEU19 VAL20 ASN21 LEU22 TYR23 LEU24 ARG25 ALA26 SER27 TYR28 THR29 TYR30 LEU31 SER32 LEU33 GLY34 PHE35

(b)

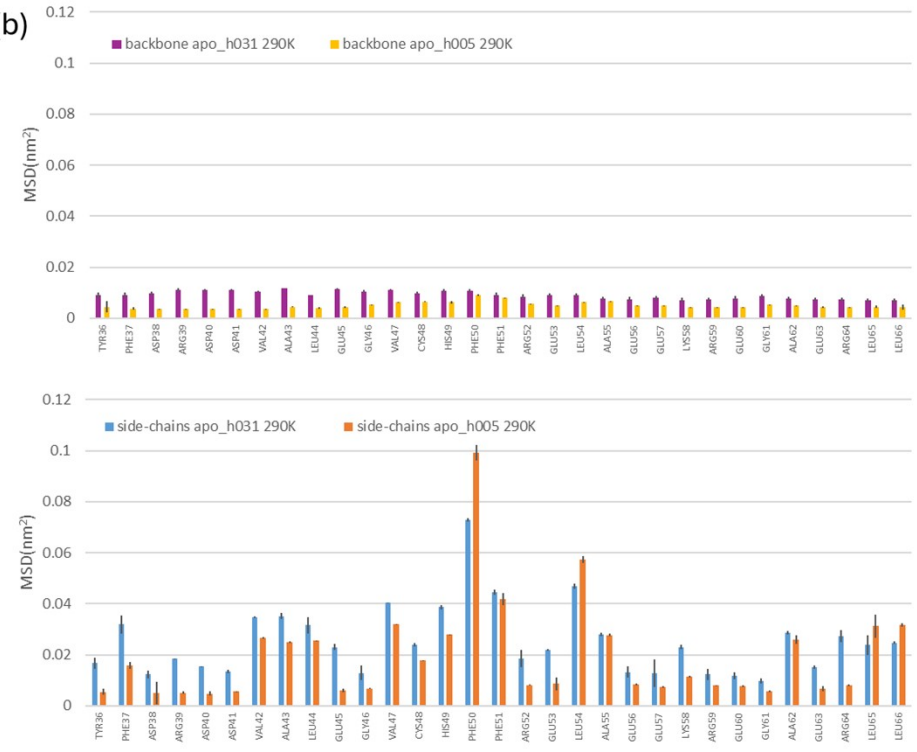
backbone apo_h031 290K
backbone apo_h005 290K
MSD(nm²)
0.12
0.1
0.08
0.06
0.04
0.02
0
TYR36 PHE37 ASP38 ARG39 ASP40 ASP41 VAL42 ALA43 LEU44 GLU45 GLY46 VAL47 CYS48 HIS49 PHE50 PHE51 ARG52 GLU53 LEU54 ALA55 GLU56 GLU57 LYS58 ARG59 GLU60 GLY61 ALA62 GLU63 ARG64 LEU65 LEU66
side-chains apo_h031 290K
side-chains apo_h005 290K
MSD(nm²)
0.12
0.1
0.08
0.06
0.04
0.02
0
TYR36 PHE37 ASP38 ARG39 ASP40 ASP41 VAL42 ALA43 LEU44 GLU45 GLY46 VAL47 CYS48 HIS49 PHE50 PHE51 ARG52 GLU53 LEU54 ALA55 GLU56 GLU57 LYS58 ARG59 GLU60 GLY61 ALA62 GLU63 ARG64 LEU65 LEU66

(c)

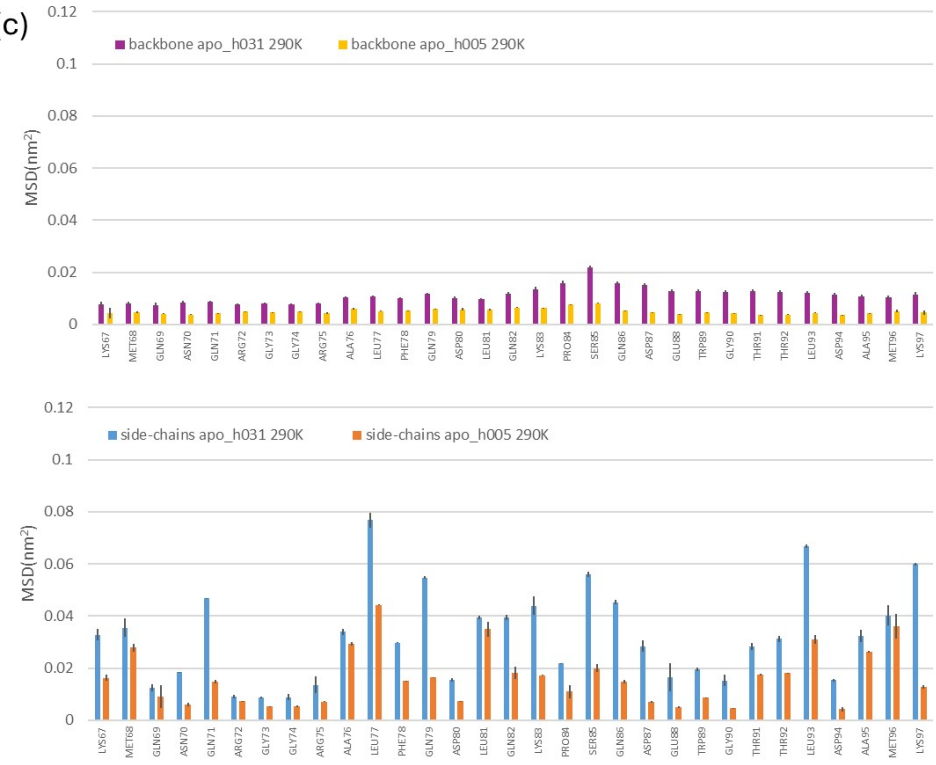
backbone apo_h031 290K
backbone apo_h005 290K
MSD(nm²)
0.12
0.1
0.08
0.06
0.04
0.02
0
LYS67 MET68 GLN69 ASN70 GLN71 ARG72 GLY73 GLY74 ARG75 ALA76 LEU77 PHE78 GLN79 ASP80 LEU81 GLN82 LYS83 PRO84 SER85 GLN86 ASP87 GLU88 TRP89 GLY90 THR91 THR92 LEU93 ASP94 ALA95 MET96 LYS97
side-chains apo_h031 290K
side-chains apo_h005 290K
MSD(nm²)
0.12
0.1
0.08
0.06
0.04
0.02
0
LYS67 MET68 GLN69 ASN70 GLN71 ARG72 GLY73 GLY74 ARG75 ALA76 LEU77 PHE78 GLN79 ASP80 LEU81 GLN82 LYS83 PRO84 SER85 GLN86 ASP87 GLU88 TRP89 GLY90 THR91 THR92 LEU93 ASP94 ALA95 MET96 LYS97

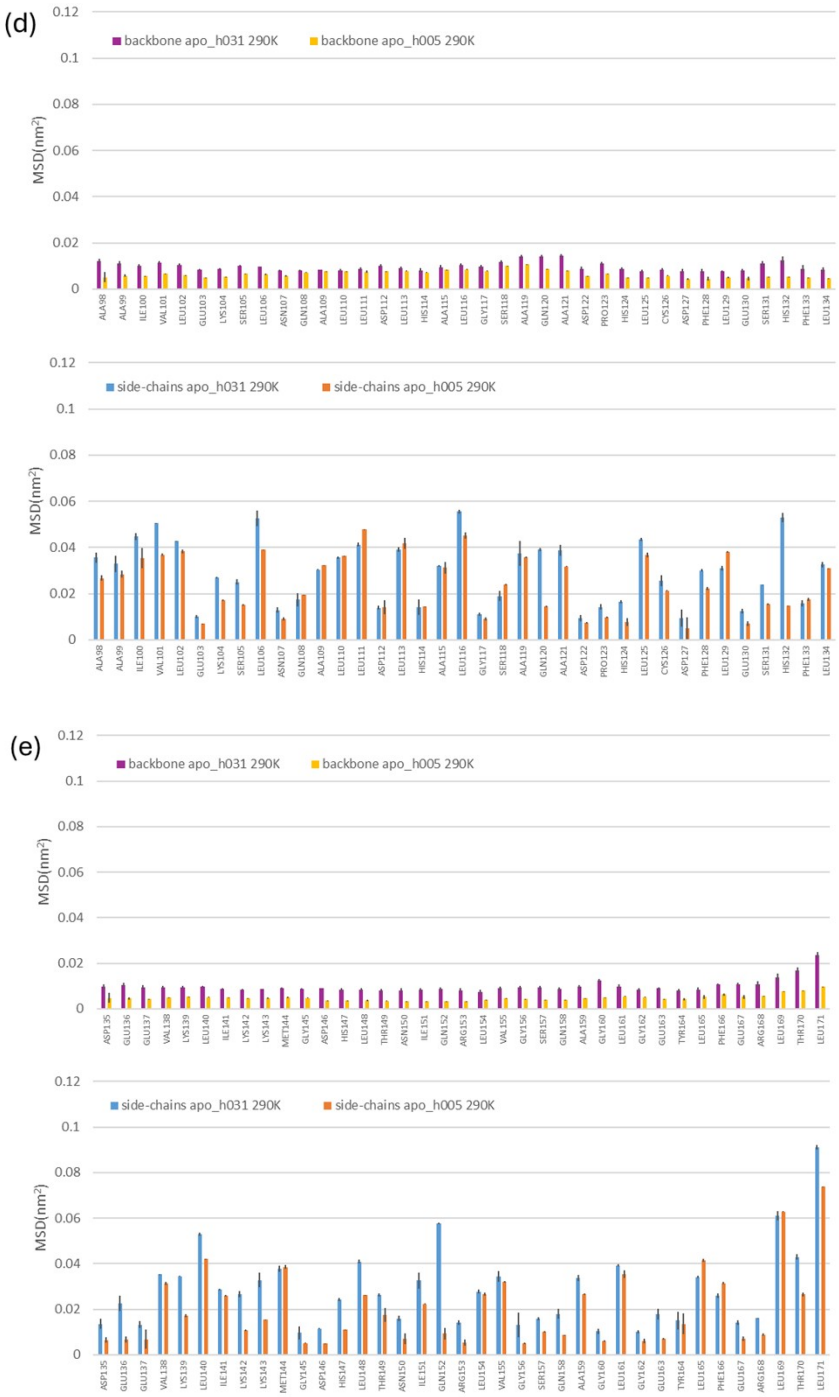

Figure SI.10. MSD per residue values for apoferritin's backbone (upper panels) and side-chain (lower panels) hydrogen atoms, in the lyophilised (apo_h005) and weakly hydrated (apo_h031) states, along the primary sequence at 290 K. Results and error bars were obtained from analysis of the last and second-to-last 10 ns of the trajectories, as averages and standard deviations, respectively. The sequence is divided into 5 regions, (a)-(e), to aid visualization.

At 150 K (Figure SI.11), in contrast to 290 K (Figure SI.10), there are several amino acids for which the MSDs of backbone and side chain are comparable. This result suggests a dynamical coupling between these residue components. The hydration-induced hindering, as shown by the greater MSD values of the dry system, in some hydrophobic residues is more accentuated for side chains, as compared to backbone (for example in ALA14, PHE50, LEU93, ALA109).

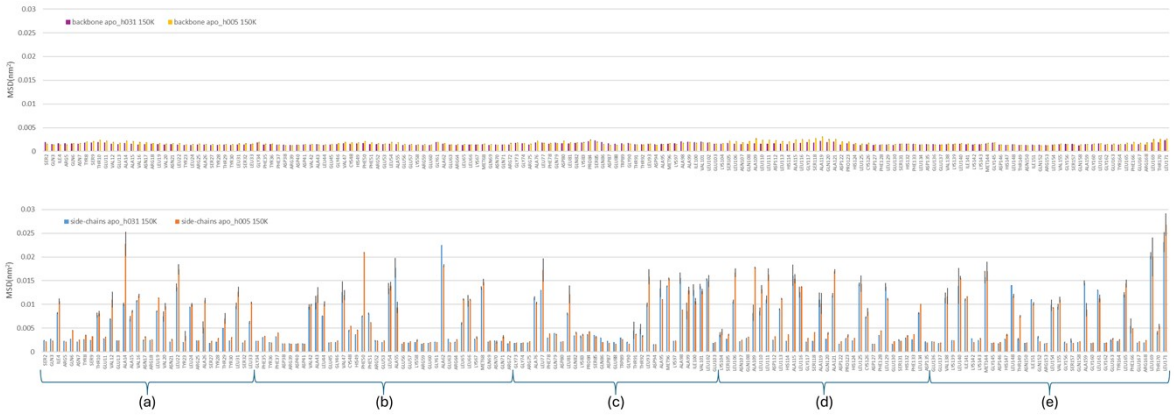

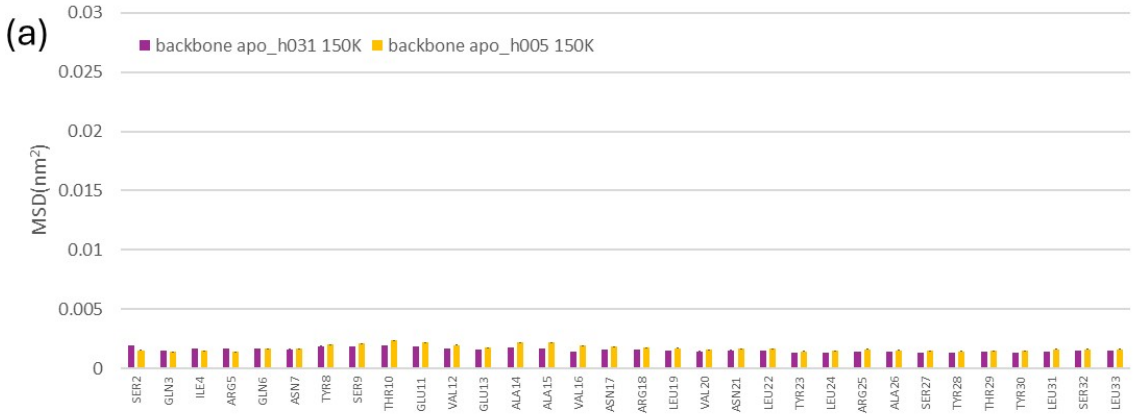

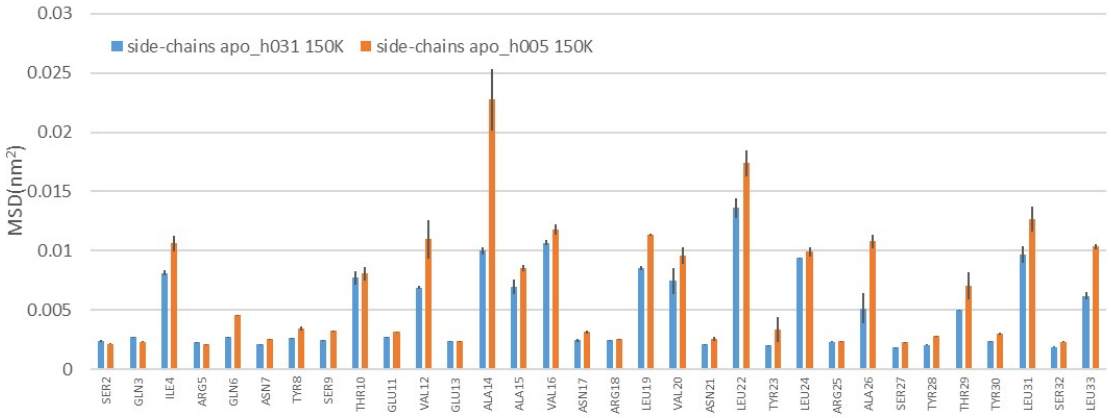

(b)

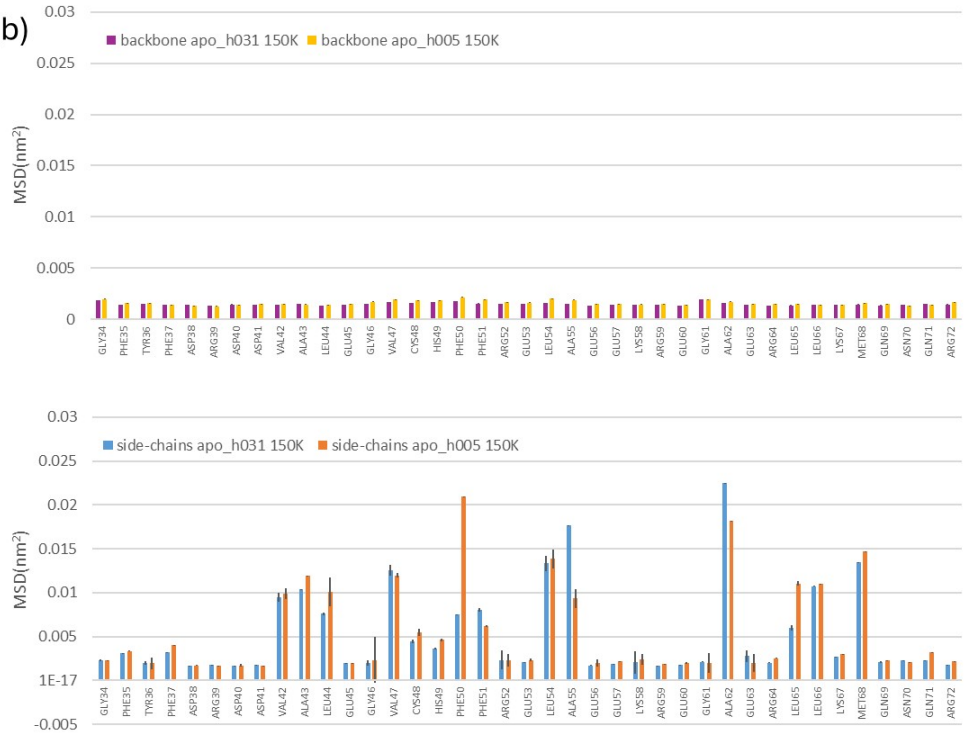
backbone apo_h031 150K
backbone apo_h005 150K
MSD(nm²)
0.03
0.025
0.02
0.015
0.01
0.005
0
GLY34 PHE35 TYR36 PHE37 ASP38 ARG39 ASP40 ASP41 VAL42 ALA43 LEU44 GLU45 GLY46 VAL47 CYS48 HIS49 PHE50 PHE51 ARG52 GLU53 LEU54 ALA55 GLU56 GLU57 LYS58 ARG59 GLU60 GLY61 ALA62 GLU63 ARG64 LEU65 LEU66 LYS67 MET68 GLN69 ASN70 GLN71 ARG72
side-chains apo_h031 150K
side-chains apo_h005 150K
MSD(nm²)
0.03
0.025
0.02
0.015
0.01
0.005
1E-17
-0.005
GLY34 PHE35 TYR36 PHE37 ASP38 ARG39 ASP40 ASP41 VAL42 ALA43 LEU44 GLU45 GLY46 VAL47 CYS48 HIS49 PHE50 PHE51 ARG52 GLU53 LEU54 ALA55 GLU56 GLU57 LYS58 ARG59 GLU60 GLY61 ALA62 GLU63 ARG64 LEU65 LEU66 LYS67 MET68 GLN69 ASN70 GLN71 ARG72

(c)

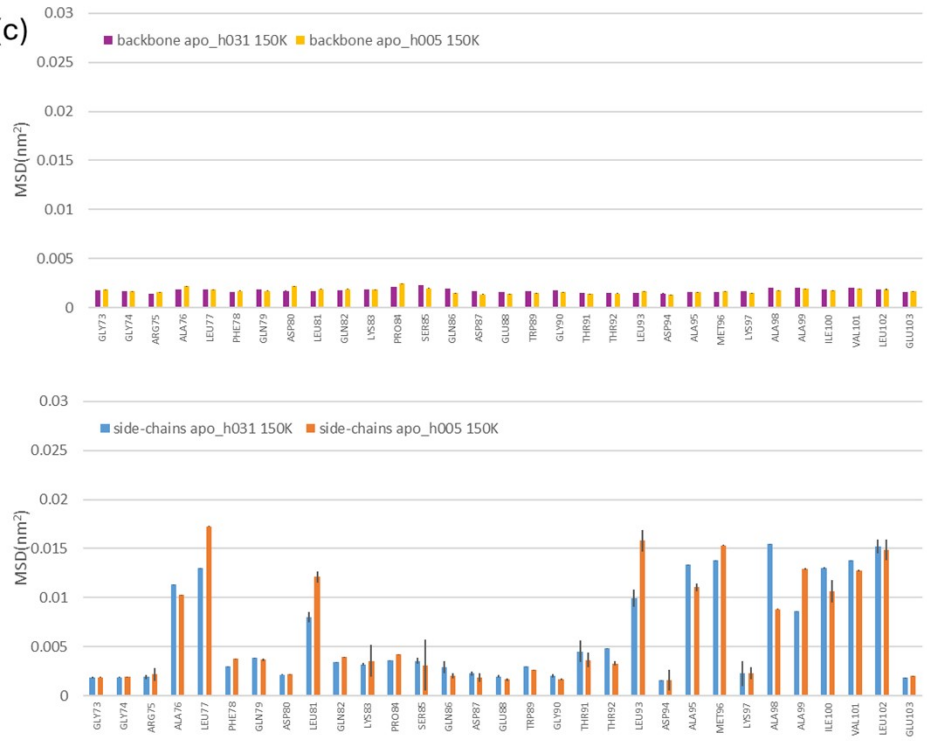
backbone apo_h031 150K
backbone apo_h005 150K
MSD(nm²)
0.03
0.025
0.02
0.015
0.01
0.005
0
GLY73 GLY74 ARG75 ALA76 LEU77 PHE78 GLN79 ASP80 LEU81 GLN82 LYS83 PRO84 SER85 GLN86 ASP87 GLU88 TRP89 GLY90 THR91 THR92 LEU93 ASP94 ALA95 MET96 LYS97 ALA98 ALA99 ILE100 VAL101 LEU102 GLU103
side-chains apo_h031 150K
side-chains apo_h005 150K
MSD(nm²)
0.03
0.025
0.02
0.015
0.01
0.005
0
GLY73 GLY74 ARG75 ALA76 LEU77 PHE78 GLN79 ASP80 LEU81 GLN82 LYS83 PRO84 SER85 GLN86 ASP87 GLU88 TRP89 GLY90 THR91 THR92 LEU93 ASP94 ALA95 MET96 LYS97 ALA98 ALA99 ILE100 VAL101 LEU102 GLU103

Figure SI.11. MSD per residue values for apoferritin's backbone (upper panels) and side-chain (lower panels) hydrogen atoms, in the lyophilised (apo_h005) and weakly hydrated (apo_h031) states, along the primary sequence at 150 K. Results and error bars were obtained from analysis of the last and second-to-last 10 ns of the trajectories, as averages and standard deviations, respectively. The sequence is divided into 5 regions, (a)-(e), to aid visualization.

SI.3.2 Distributions of backbone and side chain mobility changes

The change in mobility (%) upon hydration (Eq. 3 of the main text) for each residue was calculated separating out backbone and side-chain contributions at 150 K and 290 K. The resulting distributions at 290 K and 150 K are reported in Figure SI.12.

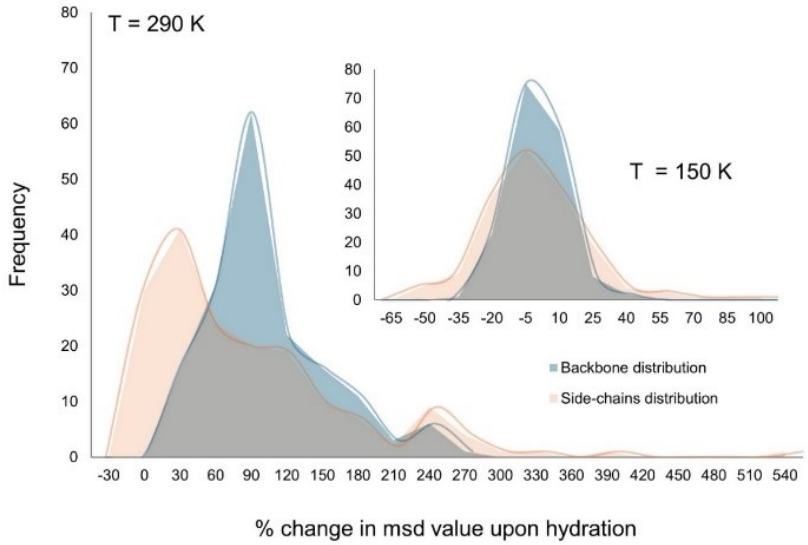

Figure SI.12. T = 290 K. Distribution of change in mobility upon hydration per residue values (Eq. 3 of main text) for backbone (blue) and side-chain (orange) hydrogen atoms. Inset: T = 150 K. Distribution of change in mobility upon hydration per residue values (Eq. 3 of main text) for backbone (blue) and side-chain (orange) hydrogen atoms.

SI.4 Backbone and Side Chain hydration analysis

The hydration of apoferritin's backbone and side-chain atoms was studied by calculating separately the Solvent Accessible Surface Area (SASA), the degree of hydration (number of water molecules within a 0.35 nm radius), and the protein-water hydrogen bonding for each group of atoms at 290 and 150 K. SASA analysis was performed for both hydration states (Figure SI.13), whilst hydration and hydrogen bonding analyses (Figures SI.14 and SI.15, respectively) were only performed for weakly hydrated apoferritin. Irrespective of temperature and hydration state, SASA of the side chains is much larger than

that of the backbone. However, the relative hydration of side chains vs backbone is not so accentuated (Figure SI.14), since the water content is not sufficient to saturate the protein surface; a surface populated also by hydrophobic side chains with a lower water affinity as compared to the hydrophilic backbone. The relative hydrogen bonding capability of side chains and backbone (Figure SI.15) is similar to the corresponding relative hydration. In terms of distribution of water molecules surrounding the side chains and backbone, no significant temperature dependant difference is detected. This finding shows that the different effect of hydration on protein mobility at 290 and 150 K does not depend on a different partition of water molecules between the two (side group and backbone) amino acid components.

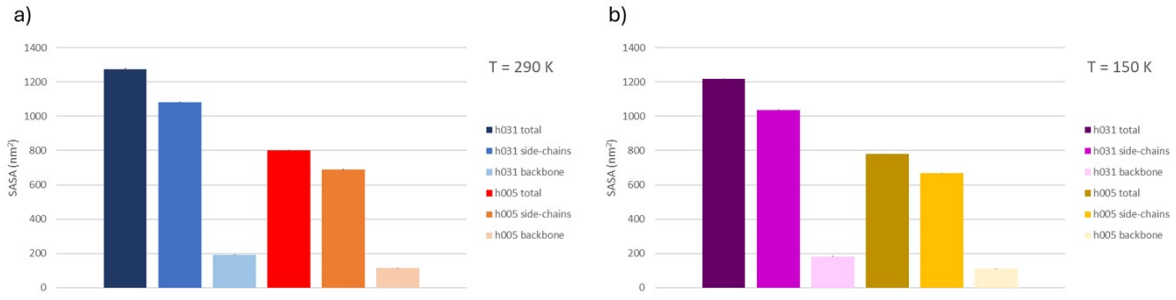

Figure SI.13. SASA (total, side-chains, backbone) of apoferritin in both hydration states at a) T = 290 K and b) T = 150 K. Results and errors were obtained from analysis of the last and second-to-last 10 ns intervals of the trajectories. Total values across the 24 subunits of the biological assembly.

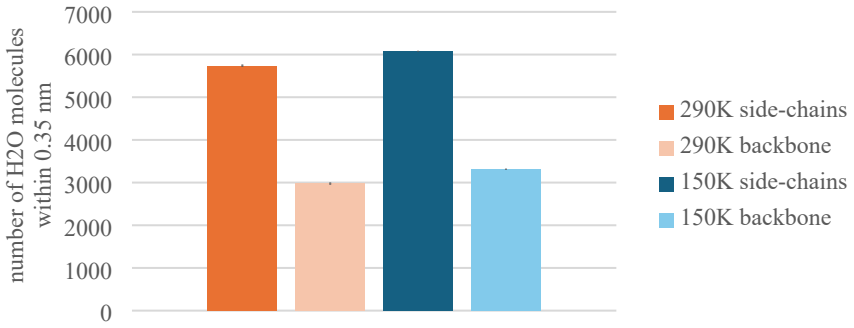

Figure SI.14. Number of H_2O molecules within a 0.35 nm radius of each atom of weakly hydrated apoferritin's backbone (muted colours) and side-chains (bright colours) at 290 K (orange) and 150 K (blue). Results and errors were obtained from analysis of the last and second-to-last 10 ns intervals of the trajectories. Total values across the 24 subunits of the biological assembly.

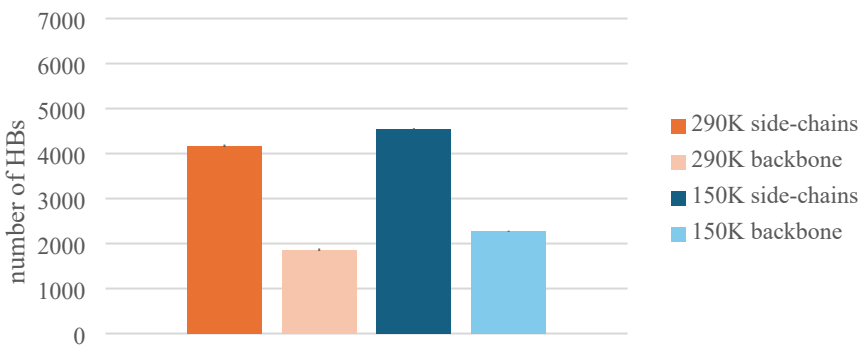

Figure SI.15. Number of hydrogen bonds formed between water and weakly hydrated apoferritin's backbone (muted colours) and water and side-chains (bright colours) at 290 K (orange) and 150 K (blue). Results and errors were obtained from analysis of the last and second-to-last 20 ns intervals of the trajectories. Total values across the 24 subunits of the biological assembly.

SI.5 Protein-water hydrogen bond lifetimes

The characteristic lifetimes, τ_H, of protein-water hydrogen bonds, obtained as described in Section SI.1.5 and used for the Arrhenius plot in the inset of Figure 9 (main manuscript), are reported in Table SI.5.

Table SI.5. Characteristic lifetime, τ_H, of protein-water hydrogen bonds in the temperature range 237.5-290 K.

T (K)	τ_H (ps)
290	255±5
280	440±15
272.5	700±5
265	1030±5
250	2615±70
237.5	5888±143

SI.6 Surface-/water- exposure and mobility effects

Surface and water exposure of apoferritin's residues were explored by calculating the SASA and the hydration degree (measured by means of the number of water molecules within a 0.35 nm radius, which approximates the thickness of the water first coordination shell surrounding a hydrophilic moiety) at a single residue level. These parameters were computed for each of the 170 amino acids at 290 and 150 K, averaging the results over the 24 subunits of the biological assembly.
To better understand the relationship between surface-/water- exposure and the local mobility effects observed, amino acids were classified as:

- Class i): surface-exposed AND significantly hydrated
- Class ii): buried OR scarcely hydrated

A dual parametrisation was adopted on the grounds that SASA-only characterisation can be misleading for the system under study in terms of hydration-induced effects. Residues were therefore classified according to both the number of water molecules within a 0.35 nm radius and their SASA. A residue belongs to class i) when the number of water molecules surrounding it exceeds the average value over all residues and the SASA is greater than the value corresponding to the intersection of the average value of water molecules per residue with the linear trend for the number of water molecules as a function of SASA. Residues that do not meet these criteria fall into class ii). Such classification is illustrated in Figures SI.16a and SI.17a for the results at 290 K and 150 K, respectively.

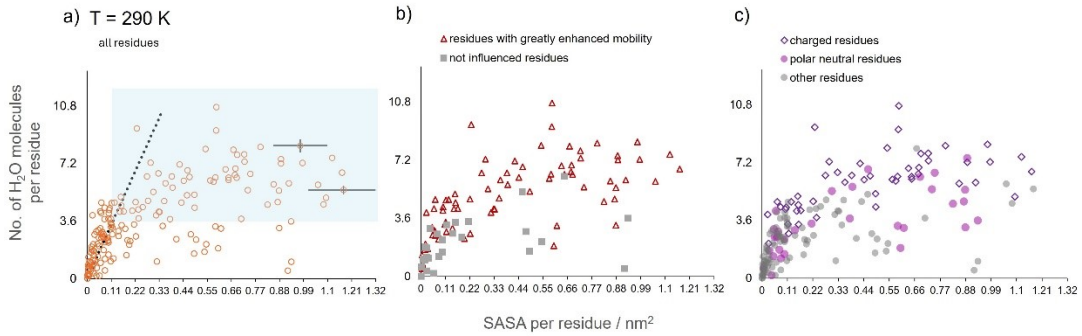

Figure SI.16. Number of H_2O molecules within a 0.35 nm radius of each atom of a residue as a function of the SASA of that residue at 290 K for weakly hydrated apoferritin. Average values over the 24 subunits and time. a) Data for all residues. Residues belonging to class i) are those falling in the top-right part of the plot (shaded box area). The dotted line represents the correlation between SASA and a residue's degree of hydration, which is expected for proteins in solution but only holds at low SASA values in a weakly hydrated system. To aid visualization, only representative error bars (showing the minimum and maximum size of the error bar for each observable) are included; errors are standard deviations over the last 10 ns of the trajectory. b) Data for residues with greatly enhanced mobility (red) and not influenced residues (grey) with respect to the dry system. c) Data for charged residues, polar neutral residues, and all other residues.

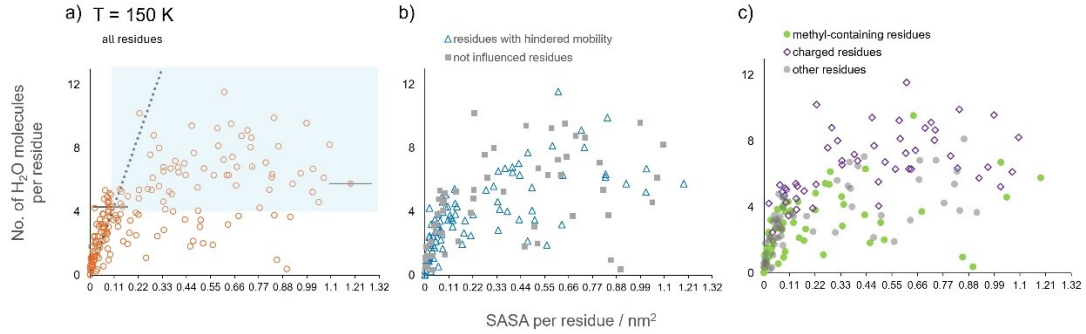

Figure SI.17. Number of H_2O molecules within a 0.35 nm radius of each atom of a residue as a function of the SASA of that residue at 150 K for weakly hydrated apoferritin. Average values over the 24 subunits and time. a) Data for all residues. Residues belonging to class i) are those falling in the top-right part of the plot (shaded box area). The dotted line represents the correlation between SASA and a residue's degree of hydration, which is expected for proteins in solution but only holds at low SASA values in a weakly hydrated system. To aid visualization, only representative error bars (showing the minimum and maximum size of the error bar for each observable) are included; errors are standard deviations over the last 10 ns of the trajectory. b) Data for residues with hindered mobility (blue) and not influenced residues (grey) with respect to the dry system. c) Data for methyl-containing residues, charged residues, and all other residues.

The findings of the MSD per residue analysis were then elaborated by distinguishing between the above defined classes of residues in terms of, first, hydration-induced mobility effect (Tables SI.6 and SI.8) and, subsequently, hydration-induced mobility effect and chemical characteristics (Tables SI.7 and SI.9). The key result is that by using this multi-parameter approach a direct influence of water proximity on protein mobility at 290 K, which is missing at 150 K, is confirmed.

Tables SI.6 and SI.7 report results of the MSD per residues analysis at 290 K, classifying residues according to water-induced effect on mobility, water- and surface-exposure, and amino acid class. Dividing residues into water- and surface-exposed (class i)) and not water-exposed or buried (class ii) gave additional insights into results presented in Tables 3 and 4 (main text). While residues of class ii) experience, to some extent, all different kinds of hydration-induced effects, virtually all residues of class i) show mobility enhancement upon hydration, with most of these belonging to the class of residues exhibiting greatly enhanced mobility (Table SI.6). Great mobility enhancement arises primarily from charged amino acids of class i) (Table SI.7), with the second greatest contribution coming from polar neutral amino acids evenly distributed between class i) and class ii).

Table SI.6. Number of class i) and class ii) residues experiencing hindrance, negligible effect, moderate enhancement and great enhancement of mobility upon hydration at 290 K in the apoferritin subunit (total number of residues = 170). Results are obtained averaging MSD per residue values over all 24 subunits. Errors are generated by analysing the last and second-to-last 10 ns intervals of the trajectory and determining a standard deviation (SD). Where errors are not reported, SD = 0 (indicating that the analysis on the two production runs gave identical results).

T = 290 K	*Water- AND surface-exposed residues: class i) (number)*	*Buried OR not water-exposed residues: class ii) (number)*
hindrance	0	12 ± 2
negligible effect	2	26 ± 2
moderate enhancement	17 ± 3	36 ± 1
great enhancement	49 ± 3	28 ± 5

Table SI.7. Contribution of each amino acid category (methyl-containing, charged, polar neutral, aromatic, aliphatic but not methyl-containing) to each hydration-induced effect (hindrance, negligible effect, moderate enhancement, great enhancement) at 290 K. The number of class i) and class ii) residues belonging to each category and showing a certain hydration-induced effect in the apoferritin subunit (total number of residues = 170) is reported. Results are obtained averaging MSD per residue values over all 24 subunits. Errors are generated by analysing the last and second-to-last 10 ns intervals of the trajectory and determining a standard deviation (SD). Where errors are not reported, SD = 0 (indicating that the analysis on the two production runs gave identical results).

T = 290 K	*methyl-containing (class i)*	*methyl-containing (class ii)*	*charged (class i)*	*charged (class ii)*	*polar neutral (class i)*	*polar neutral (class ii)*	*aromatic (class i)*	*aromatic (class ii)*	*aliphatic, non-CH3 (class i)*	*aliphatic, non-CH3 (class ii)*
hindrance	*0*	*9 ± 2*	*0*	*0*	*0*	*1*	*0*	*2*	*0*	*0*
negligible effect	*1*	*16 ± 1*	*1*	*1*	*0*	*4 ± 1*	*0*	*5*	*0*	*0*
moderate enhancement	*7 ± 1*	*23 ± 2*	*7 ± 2*	*3 ± 1*	*2 ± 1*	*6*	*1 ± 1*	*1 ± 1*	*0*	*3 ± 2*
great enhancement	*4 ± 1*	*1 ± 1*	*33 ± 1*	*5 ± 1*	*9 ± 1*	*9 ± 1*	*1 ± 1*	*5 ± 1*	*2*	*8 ± 2*

Tables SI.8 and SI.9 summarize the results of the same analysis for the temperature of 150 K. Data presented in Table SI.8 reveal that low-temperature mobility hindrance primarily arises from buried or not water-exposed residues, while other effects are observed equally in species of both class i) and ii). In particular, water appears to hinder primarily class ii) residues, with the greatest contribution to this effect coming from class ii) methyl-containing residues (Table SI.9); the only amino acid category that predominantly experiences hindrance when hydrated and surface-exposed is the one of charged residues, which contribute the second greatest amount to this effect.

Table SI.8. Number of class i) and class ii) residues experiencing hindrance, negligible effect, moderate enhancement and great enhancement of mobility upon hydration at 150 K in the apoferritin subunit (total number of residues = 170). Results are obtained averaging MSD per residue values over all 24 subunits. Errors are generated by analysing the last and second-to-last 10 ns intervals of the trajectory and determining a standard deviation (SD). Where errors are not reported, SD = 0 (indicating that the analysis on the two production runs gave identical results).

T = 150 K	*Water- AND surface-exposed residues: class i) (number)*	*Buried OR not water-exposed residues: class ii) (number)*
hindrance	30 ± 1	61 ± 1
negligible effect	24 ± 1	30 ± 1
moderate enhancement	11 ± 1	12 ± 1
great enhancement	1 ± 1	1

Table SI.9. Contribution of each amino acid category (methyl-containing, charged, polar neutral, aromatic, aliphatic but not methyl-containing) to each hydration-induced effect (hindrance, negligible effect, moderate enhancement, great enhancement) at 150 K. The number of class i) and class ii) residues belonging to each category and showing a certain hydration-induced effect in the apoferritin subunit (total number of residues = 170) is reported. Results are obtained averaging MSD per residue values over all 24 subunits. Errors are generated by analysing the last and second-to-last 10 ns intervals of the trajectory and determining a standard deviation (SD). Where errors are not reported, SD = 0 (indicating that the analysis on the two production runs gave identical results).

T = 150 K	*methyl-containing (class i)*	*methyl-containing (class ii)*	*charged (class i)*	*charged (class ii)*	*polar neutral (class i)*	*polar neutral (class ii)*	*aromatic (class i)*	*aromatic (class ii)*	*aliphatic, non-CH3 (class i)*	*aliphatic, non-CH3 (class ii)*
hindrance	*8 ± 1*	*26 ± 1*	*16 ± 1*	*7 ± 1*	*5 ± 1*	*13 ± 1*	*1*	*10 ± 1*	*0*	*5 ± 1*
negligible effect	*4*	*13 ± 1*	*18 ± 1*	*4 ± 1*	*1 ± 1*	*5 ± 2*	*0*	*2 ± 1*	*1*	*6 ± 1*
moderate enhancement	*0*	*8 ± 1*	*5*	*0*	*5 ± 1*	*2 ± 1*	*0*	*2 ± 1*	*1*	*0*
great enhancement	*1 ± 1*	*1*	*0*	*0*	*0*	*0*	*0*	*0*	*0*	*0*

SI.7 Structural characterisation of water molecules in weakly hydrated apoferritin

SI.7.1 Water-water hydrogen bonds distributions

The possibility of the low-temperature hindrance effect being due to local formation of ice was explored by considering the distribution of the number of water-water hydrogen bonds per water molecule in the weakly hydrated system at 290 K and 150 K (Figure SI.18).

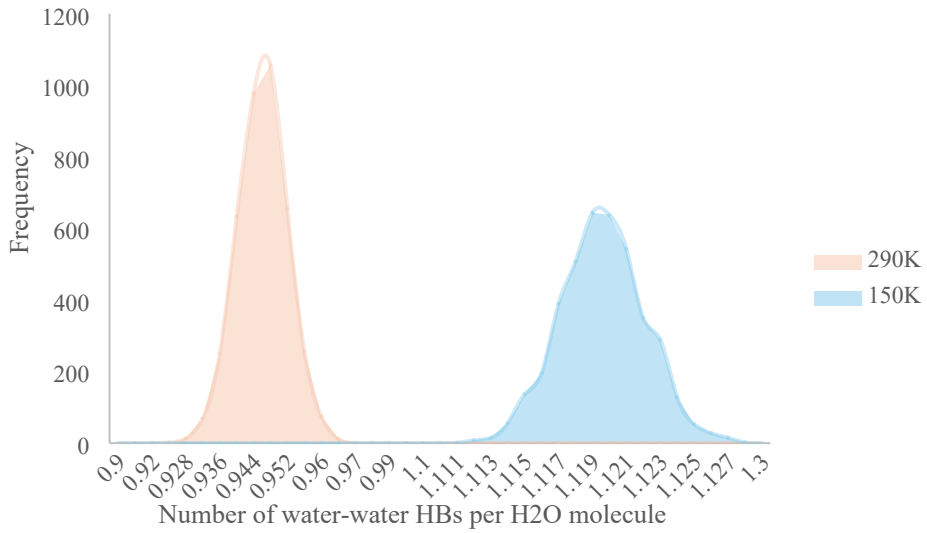

Figure SI.18. Distributions of number of water-water hydrogen bonds per H_2O molecule over the last 20 ns of the trajectory at T=290K (orange) and T=150K (blue).

As expected, the connectivity between water molecules is lower at the highest temperature. More interestingly, the upper number of hydrogen bonds per water molecule at 150 K is much lower than 2, i.e., the value expected for a tetracoordinated water molecule in ice. This finding rules out the formation, and presence, of ice nuclei.

SI.7.2 Water cluster size distribution

To detect a possible influence of the distribution of water molecules on protein mobility, the water cluster size distribution in the weakly hydrated system was determined at 290 K and 150 K (Figure SI.19).

The number of clusters formed by water molecules was calculated using as the clustering criterium a distance between oxygen atoms of water molecules less than 0.35 nm.

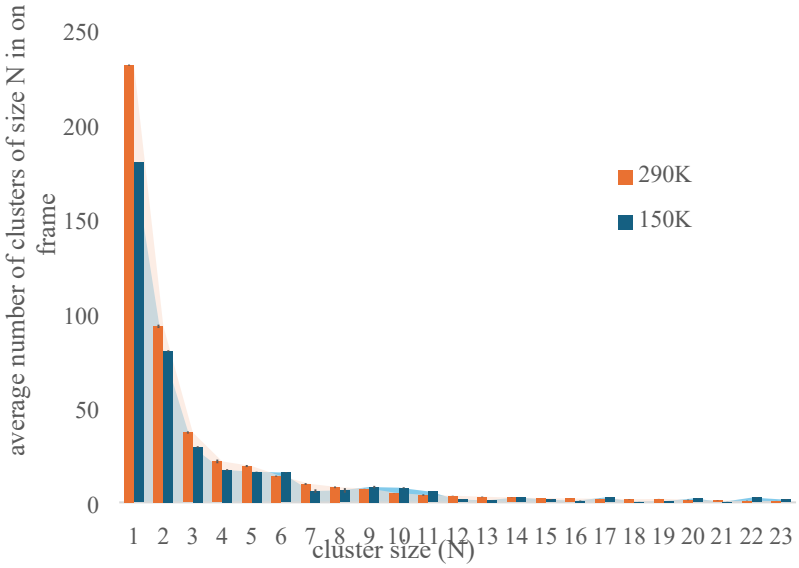

Figure SI.19. Average number of water-molecule clusters of size N in one frame as a function of cluster size (N) at T = 290 K (orange) and T = 150 K (blue). Results and errors are averages and standard deviations from analysis of the last and second-to-last 10 ns intervals of each trajectory, respectively.

Results presented in Figure SI.19 show that the majority of water molecules exist either as single molecules or form clusters comprised of only a few molecules. Populations of large clusters (N>20) is negligible.

SI.7.3 Protein-water hydrogen bond networks

The presence of hydrogen bond networks between water and protein atoms in weakly hydrated apoferritin at 150 K was examined in proximity of those apoferritin channels where some hindered residues are located. For instance, residue ASP 112, which forms the highest number of persistent hydrogen bonds with water (Figure SI.22a) and is located in the 3-fold channel, was found to participate in a hydrogen bond/dipolar interaction network. This network includes water molecules and atoms of ASP 112 and neighbouring residues, connected by hydrogen bonds and dipolar interactions (Figure SI.20). Such connectivity is probably involved in the water-induced hindering effect of this region.

However, this is not a common feature in the system, since only a small (∼5%) fraction of all amino acids characterised by both high water exposure and strong residue-water interaction (i.e., a significantly high number of HBs) is directly hindered by water proximity.

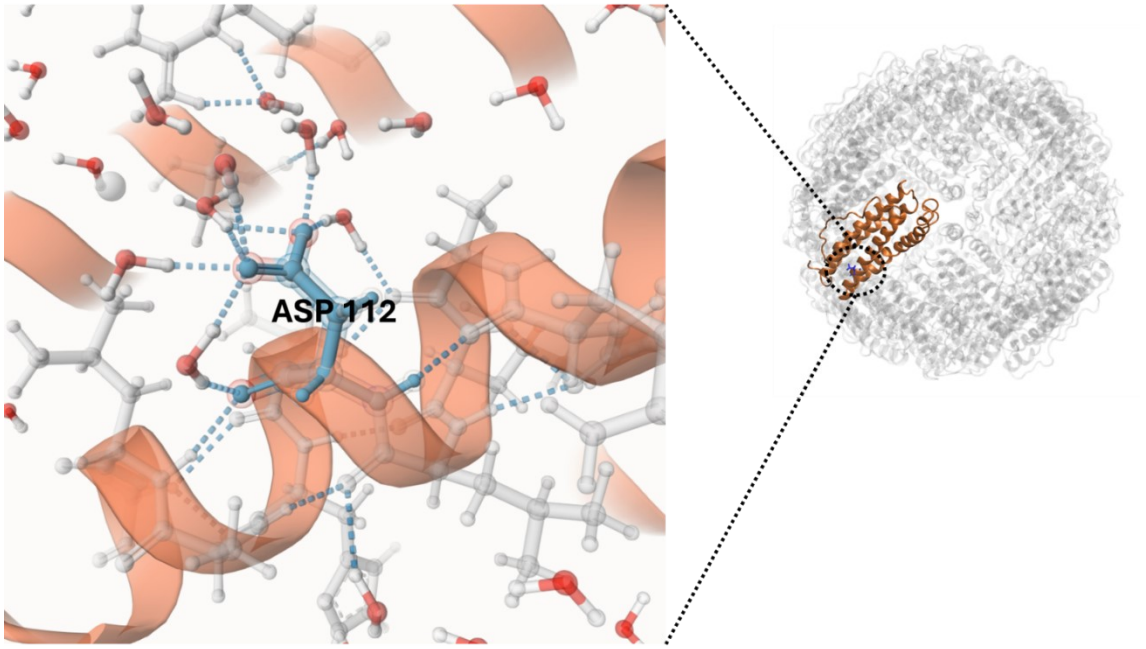

Figure SI.20. Snapshot of the surroundings of ASP112 (blue) in the subunit highlighted in orange. Other residues are represented in light grey, water molecules are red (oxygens) and white (hydrogens); the α-helices are coloured in orange. Dipolar and hydrogen bond interactions are represented as light blue dotted lines. T = 150 K. The first frame of the last 20 ns production run, used for hydrogen bonds analysis, was chosen for visualization.

SI.8 Protein-water hydrogen bonds per residue

Panels (a)-(d) of Figures 10 and 11 in the main text, which report the number of protein-water hydrogen bonds formed by each residue for more than 20% of the 290 K and 150 K 10 ns trajectories, are shown in Figures SI.21 and SI.22 for improved readability.

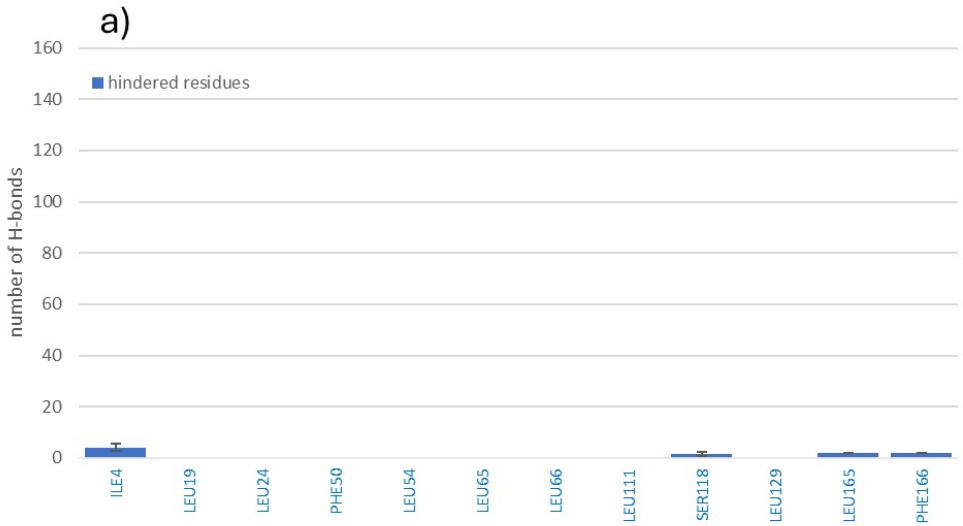
a)
hindered residues
number of H-bonds
0
20
40
60
80
100
120
140
160
ILE4
LEU19
LEU24
PHE50
LEU54
LEU65
LEU66
LEU111
SER118
LEU129
LEU165
PHE166

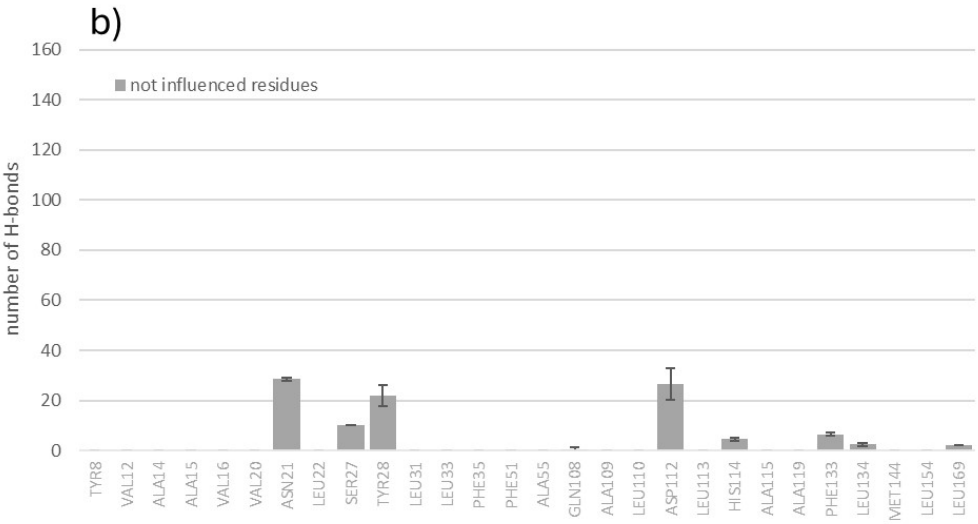
b)
not influenced residues
number of H-bonds
0
20
40
60
80
100
120
140
160
TYR8
VAL12
ALA14
ALA15
VAL16
VAL20
ASN21
LEU22
SER27
TYR28
LEU31
LEU33
PHE35
PHE51
ALA55
GLN108
ALA109
LEU110
ASP112
LEU113
HIS114
ALA115
ALA119
PHE133
LEU134
MET144
LEU154
LEU169

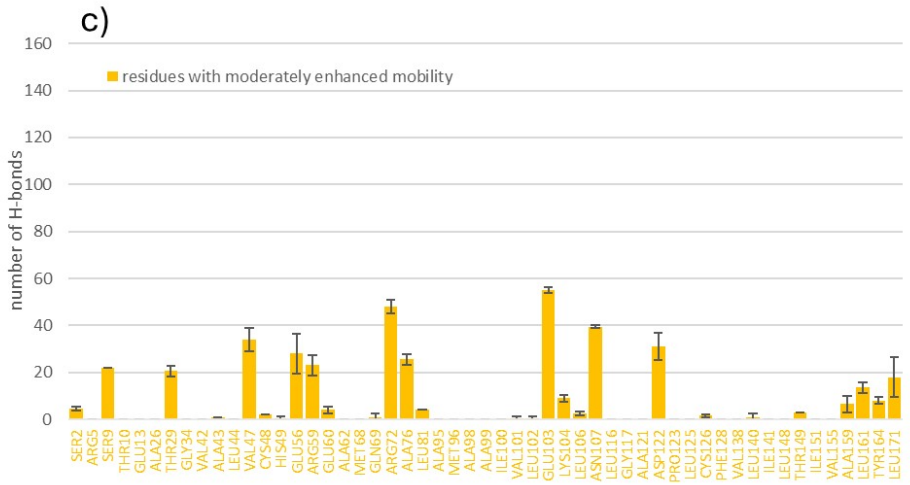
c)
residues with moderately enhanced mobility
number of H-bonds
0
20
40
60
80
100
120
140
160
SER2
ARG5
SER9
THR10
GLU13
ALA26
THR29
GLY34
VAL42
ALA43
LEU44
VAL47
CYS48
HIS49
GLU56
ARG59
GLU60
ALA62
MET68
GLN69
ARG72
ALA76
LEU81
ALA85
MET96
ALA98
ALA99
ILE100
VAL101
LEU102
GLU103
LYS104
LEU106
ASN107
LEU116
GLY117
ALA121
ASP122
PRO123
LEU125
CYS126
PHE128
VAL138
LEU140
ILE141
LEU148
THR149
ILE151
VAL155
ALA159
LEU161
TYR164
LEU171

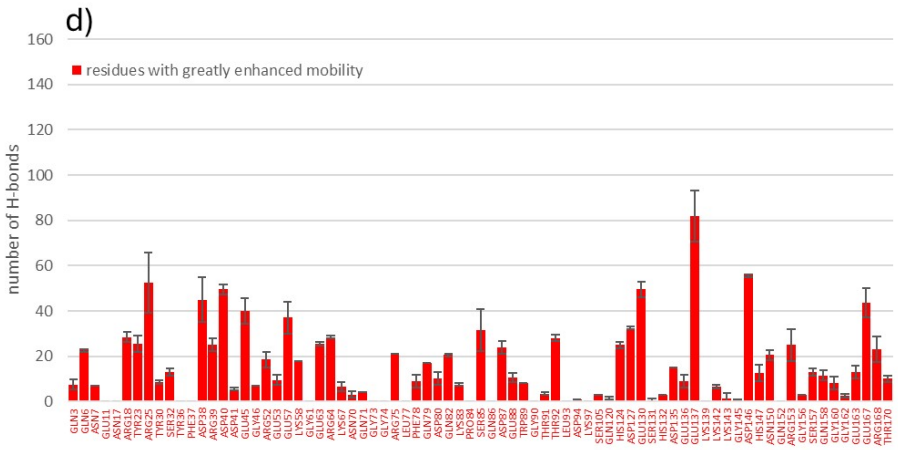

Figure SI.21. Number of hydrogen bonds formed for at least 20% of the trajectory (even non-continuously) at 290 K by amino acids experiencing a) hindrance, b) no effect, c) moderate enhancement of the mobility, d) great enhancement of the mobility upon hydration. Each panel displays results specific to a particular class of amino acids, with x-ticks representing only residues within that class. Note that x-ticks without corresponding bars indicate amino acids that did not form hydrogen bonds. Results and errors are averages and standard deviations over the last and second-to-last 10 ns intervals of each trajectory, respectively.

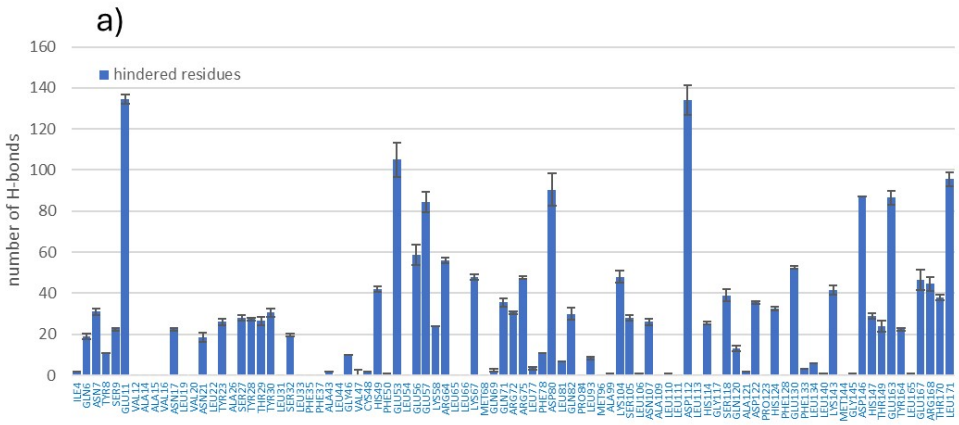
a)
hindered residues
number of H-bonds
0
20
40
60
80
100
120
140
160

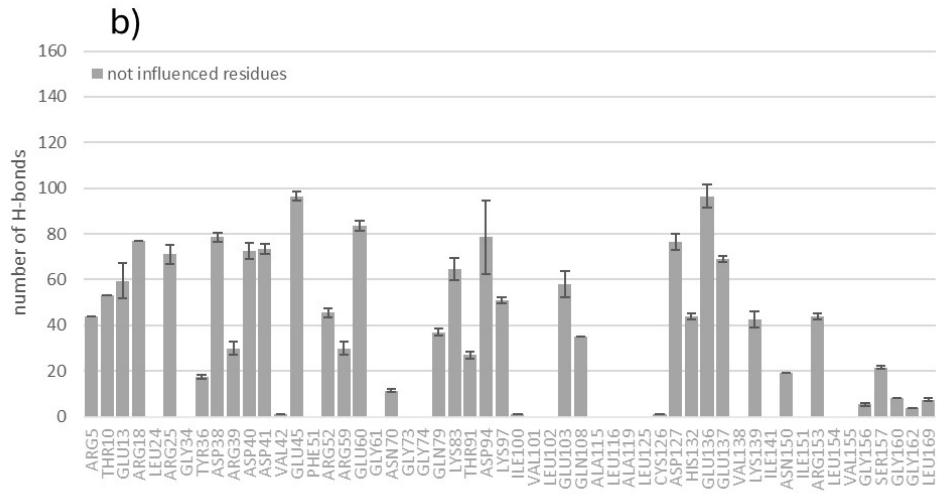
b)
not influenced residues
number of H-bonds
0
20
40
60
80
100
120
140
160
ARG5
THR10
GLU13
ARG18
LEU24
ARG25
GLY34
TYR36
ASP38
ARG39
ASP40
ASP41
VAL42
GLU45
PHE51
ARG52
ARG59
GLU60
GLY61
ASN70
GLY73
GLY74
GLN79
LYS83
THR91
ASP94
LYS97
ILE100
VAL101
LEU102
GLU103
GLN108
ALA115
LEU116
ALA119
LEU125
CYS126
ASP127
HIS132
GLU136
GLU137
VAL138
LYS139
ILE141
ASN150
ILE151
ARG153
LEU154
VAL155
GLY156
SER157
GLY160
GLY162
LEU169

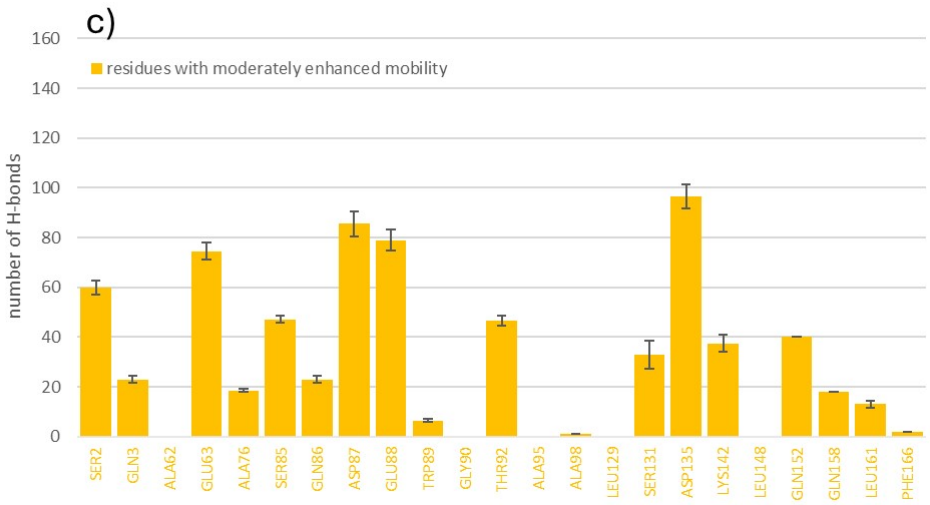
c)
residues with moderately enhanced mobility
number of H-bonds
0
20
40
60
80
100
120
140
160
SER2
GLN3
ALA62
GLU63
ALA76
SER85
GLN86
ASP87
GLU88
TRP89
GLY90
THR92
ALA95
ALA98
LEU129
SER131
ASP135
LYS142
LEU148
GLN152
GLN158
LEU161
PHE166

Figure SI.22. Number of hydrogen bonds formed for at least 20% of the trajectory (even non-continuously) at 150 K by amino acids experiencing a) hindrance, b) no effect, c) moderate enhancement of the mobility, d) great enhancement of the mobility upon hydration. Each panel displays results specific to a particular class of amino acids, with x-ticks representing only residues within that class. Note that x-ticks without corresponding bars indicate amino acids that did not form hydrogen bonds. Results and errors are averages and standard deviations over the last and second-to-last 10 ns intervals of each trajectory, respectively.

SI.9 Possible factors influencing hindrance

The presence or absence of low-temperature hindrance as detected by neutron scattering experiments is likely linked to specific characteristics of the sample studied, such as chain length and hydration level, and/or to the neutron instrument's resolution (i.e. the experimental time scale probed). Table SI.10 collates information (material studied, associated chain length, number of subunits, hydration level, instrument energy resolution, and reported evidence of hindered behaviour at low temperature) from neutron scattering experiments conducted on various proteins, and across different neutron spectrometers. The data aims to help identify those factors that most likely drive the low-temperature hindrance effect observed.

Table SI.10. Information (system studied, chain length, number of subunits, hydration level, instrument resolution, and whether a hindrance effect was detected at low temperatures) on neutron scattering experiments

conducted on various proteins, and across different instruments, to investigate hydration-induced effects on mobility.

protein	*chain length*	*number of subunits*	*hydration level*	*resolution FWHM (μeV)*	*instrument*	*hindrance detected*
apoferritin[1]	174	24	0.31	24.5	OSIRIS	yes
GFP[4]	238	2	0.4	1	NG2	yes
pig liver esterase[5]	566	5	0.5	100	IN5	yes
lysozyme[6,7]	147	1	0.4	1/8	IN10/IN13	yes/yes
RNAse A[8]	124	1	0.4	0.9/100	IN16/IN5	yes/no
myoglobin[9]	154	1	0.2	8	IN13	no
homopolypeptides[10]	~50-100	N/A	0.2	8	IN13	no
insulin[1]	51	2	0.25	17.5	IRIS	no

References

1 E. Bassotti, S. Gabrielli, G. Paradossi, E. Chiessi and M. Telling, *Commun Chem*, 2024, **7**, 83.

2 N. Michaud-Agrawal, E. J. Denning, T. B. Woolf and O. Beckstein, *Journal of Computational Chemistry*, 2011, **32**, 2319–2327.

3 R. J. Gowers, M. Linke, J. Barnoud, T. J. E. Reddy, M. N. Melo, S. L. Seyler, J. Domański, D. L. Dotson, S. Buchoux, I. M. Kenney and O. Beckstein, *Proceedings of the 15th Python in Science Conference*, 2016, 98–105.

4 J. D. Nickels, H. O'Neill, L. Hong, M. Tyagi, G. Ehlers, K. L. Weiss, Q. Zhang, Z. Yi, E. Mamontov, J. C. Smith and A. P. Sokolov, *Biophysical Journal*, 2012, **103**, 1566–1575.

5 V. Kurkal, R. M. Daniel, J. L. Finney, M. Tehei, R. V. Dunn and J. C. Smith, *Chemical Physics*, 2005, **317**, 267–273.

6 J. H. Roh, V. N. Novikov, R. B. Gregory, J. E. Curtis, Z. Chowdhuri and A. P. Sokolov, *Phys Rev Lett*, 2005, **95**, 038101.

7 S. Magazù, F. Migliardo and A. Benedetto, *J. Phys. Chem. B*, 2011, **115**, 7736–7743.

8 K. Wood, C. Caronna, P. Fouquet, W. Haussler, F. Natali, J. Ollivier, A. Orecchini, M. Plazanet and G. Zaccai, *Chemical Physics*, 2008, **345**, 305–314.

9 G. Schirò, M. Sclafani, C. Caronna, F. Natali, M. Plazanet and A. Cupane, *Chemical Physics*, 2008, **345**, 259–266.

10 G. Schirò, C. Caronna, F. Natali and A. Cupane, *Phys. Chem. Chem. Phys.*, 2010, **12**, 10215–10220.